1.0

2.8   2.5

3.2   2.2

3.6

4.0   2.0

1.1

1.8

1.25   1.4   1.6

MICROCOPY RESOLUTION TEST CHART
NATIONAL BUREAU OF STANDARDS 1963

See

1473

OCEAN BOTTOM SEISMOMETER STUDY OF THE KURIL TRENCH AREA

By

JUNZO KASAHARA and ROBERT R. HARVEY

AUGUST 1976

HAWAII INSTITUTE OF GEOPHYSICS
UNIVERSITY OF HAWAII, HONOLULU

and

JOINT TSUNAMI RESEARCH EFFORT
PACIFIC MARINE ENVIRONMENTAL LABORATORY
ENVIRONMENTAL RESEARCH LABORATORIES, NOAA

HAWAII INSTITUTE OF GEOPHYSICS
UNIVERSITY OF HAWAII

OCEAN BOTTOM SEISMOMETER STUDY
OF THE KURIL TRENCH AREA

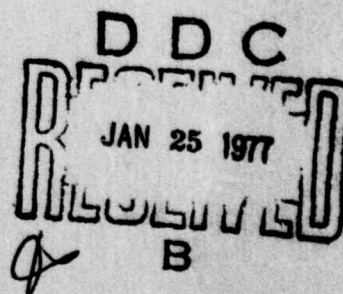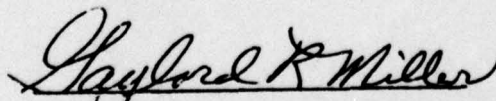By

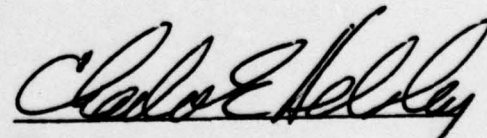Junzo Kasahara[1] and Robert R. Harvey

AUGUST 1976

Hawaii Institute of Geophysics
University of Hawaii, Honolulu

and

Joint Tsunami Research Effort
Pacific Marine Environmental Laboratory
Environmental Research Laboratories, NOAA

Director
Joint Tsunami Research Effort

Director
Hawaii Institute of Geophysics

[1]ON LEAVE FROM EARTHQUAKE RESEARCH INSTITUTE, UNIVERSITY OF TOKYO.

ABSTRACT

An ocean bottom seismograph was deployed on the seaward side of the Kuril Trench off Hokkaido, Japan in 5460 m of water, in August during the 1975 Joint Soviet-American Tsunami Expedition. During the seven-day record, S-P times were distributed in three groups: 19-24 sec, corresponding to aftershocks of the 10 June and 13 June 1975 earthquakes southeast of Nemuro, Japan and to earthquakes east of Sanriku, Japan; ~30 sec, from south of Erimo Peninsula, Hokkaido; and ~100 sec, from the Izu-Bonin Islands. Seven earthquakes, with hypocenters well determined by the land seismic net, are studied in detail. A shallow focus earthquake yields typical oceanic mantle velocities shallower than 50 km in the slab which dips under the Japanese archipelago. However, deeper focus earthquakes reveal anomalously high velocities ($V_p \geq 8.50$ km/sec, $V_s \geq 4.80$ km/sec) averaged over the upper 230 km, in agreement with the models of Utsu and Oliver and Isacks. Two deep earthquakes, whose paths lie in the Pacific Ocean asthenosphere, suggest a velocity 3% lower than that predicted by Jeffreys-Bullen, in agreement with the above models. Spectral analysis of S arrivals suggests Q_s values of 1000-1500 for nearby earthquakes (S-P < 43 sec) and 4000-6000 for longer distance earthquakes, implying an unusual attenuation mechanism for long travel paths, which enhances the high frequencies.

iii

TABLE OF CONTENTS

LIST OF TABLES

LIST OF FIGURES

17. Sonograms as recorded on Sona-Graph. Contours correspond to
    6-db amplitude intervals P, S, and T refer to P-phase, S-phase,
    and T-phase arrivals; and H and V refer to horizontal and vertical
    channels.

18. S-wave spectra for selected earthquakes, obtained as a cut through
    a sonogram at the peak in S-phase energy and corrected for the
    OBS system response. Numbers on curves refer to S-P time in seconds.

19. Q variation as a function of S-P time. The ordinate refers to the
    slope of logarithmic amplitude decay with frequency. The solid and
    dotted lines are calculated using a model with a flat velocity
    amplitude source spectrum with varying Q for P and S waves, respectively.

INTRODUCTION

The 1975 Soviet-American Tsunami Expedition intended to study tsunami generation, propagation, and runup. The program comprised a cooperative effort between scientists of the Joint Tsunami Research Effort, NOAA; Hawaii Institute of Geophysics, University of Hawaii; and the Sakhalin Complex Scientific Research Institute and the Hydrometeorological Service of the U.S.S.R. The field effort [*Soloviev, Miller* et al., 1976] involved a two-month cruise along the Pacific coast of Hokkaido and the southern Kuril Islands, during which the following free-vehicle instruments were deployed: nine bottom pressure recorders, one vertical electric field recorder, and one ocean bottom seismograph (OBS). Figure 1 shows the instrument locations. This paper reports on the analysis of the OBS data. Water wave results are being published separately [*Efimov et al.*, in press].

OBS DESCRIPTION

The OBS was built at the Hawaii Institute of Geophysics and is a modified version of that designed by the Earthquake Research Institute, University of Tokyo [*Kasahara et al.*, 1973, 1974a, 1974b; *Sutton et al.*[2]]. The instrument operates as a free vehicle and consists basically of data acquisition and recovery systems.

---

[2] SUTTON, G. H., J. KASAHARA, W. N. ICHINOSE, AND D. A. BYRNE. MS. OCEAN BOTTOM SEISMOGRAPH DEVELOPMENT AT HAWAII INSTITUTE OF GEOPHYSICS, IN PREPARATION.

Figure 2 depicts the assembled OBS. Obvious components from top to bottom are the flotation module, pressure case, release, and disposable anchor.   Flotation consists of five 10-inch diameter glass spheres which provide 8 kg of net positive buoyancy upon release of the ballast. The 18-cm outside diameter aluminum pressure vessel is fabricated of 7075-T6 alloy and is capable of resisting external pressure to 10-km water depth. Dual explosive bolts separate the anchor from the instrument package at the preset release time, which is controlled by two independent clocks. In the photograph a safety shield covers the release mechanism. Finally, a 45-kg core weight serves as ballast; the complete assembly weighs 37 kg in water and sinks at roughly 1 m/sec. Not shown in the photograph are two retrieval radio beacons with flags, which attach to the straps connecting the recorder and flotation packages.

The data acquisition system includes a two-component, 4.5-Hz velocity-type seismometer (horizontal and vertical components), gimbaled suspension, amplifiers, cassette magnetic tape recorder, and time code generator, as shown in the block diagram (Figure 3).

The seismic sensor is manufactured by Geo-Space Co., Ltd.[3] and is mounted in a gimbaled suspension, with slip rings formed from printed circuit board. The vertical signal is split to two amplifiers of 0.2-microvolt input noise with gains of 95 and 75 decibels (dB), the outputs of which feed channels one and two of the cassette

---

[3] MENTION OF A COMMERCIAL COMPANY OR PRODUCT DOES NOT CONSTITUTE AN ENDORSEMENT. USE FOR PUBLICITY OR ADVERTISING PURPOSES OF INFORMATION FROM THIS PUBLICATION CONCERNING PROPRIETARY PRODUCTS OR THE TESTS OF SUCH PRODUCTS IS NOT AUTHORIZED.

recorder. The horizontal signal is amplified by 95 dB and records on channel three. Each minute, the fourth channel receives a serial binary coded decimal (BCD) time code signal of days, hours, and minutes, superposed on a basic 1-sec-period square wave.

The cassette tape recorder is modified from the Sanyo model M1102. A 5-rpm d.c. motor (Olympus Precision Co., Ltd., model CP-5-G5) replaces the original d.c. motor. Thus a standard C-120 chromium dioxide cassette tape is driven 400 times slower than normal and lasts for up to 16 days. Also the original recording head is replaced by a four-track head made by Alps Co., Ltd. In order to shield mechanical vibration of the d.c. motor, foam rubber surrounds the cassette tape recorder. The recording system response curve is shown in Figure 4.

Release is effected by either of two identical countdown timers. In each, an electromechanical clock supplies hour pulses that activate a subtracting counter that is preset for release time in hours. When the count reaches zero, an explosive bolt drops the lead ballast, and the unit floats to the surface. Pressure deactivated radio beacons then beam a locating signal to the ship's receiver for recovery.

The playback scheme is shown in Figure 5. The chromium dioxide tape is played on a TEAC model R-70A tape deck, into a Hewlett-Packard model 3960, one-fourth inch tape recorder, and subsequently to either a Honeywell 3-kHz model 1308A Visicorder for visual seismogram recording or to a model 6061-A Sona-Graph for a spectral signature.

4

The TEAC operates at the standard 4.75 cm/sec tape speed, representing
a 400-times speedup. The Hewlett-Packard instrument records at 19 cm/sec
and plays back at 9.5 cm/sec, resulting in an effective 200-times
speedup from real time. Accordingly, the system response, including
playback elements, has the form shown in Figure 4.

The crystal-controlled BCD time code generator was cali-
brated by JJY Radio before deployment and by WWVH Radio after
retrieval. Absolute timing accuracy for the present survey was
± 0.1 sec.

S-P TIME DISTRIBUTION AND TYPICAL FEATURES

The OBS was deployed on the seaward side of the Kuril Trench
at 41.415°N, 146.417°E, in 5460 m of water (see Figure 1) on 11 August
and was retrieved on 31 August 1975.

Position was determined by loran C. The change in noise
character of the seismic record upon launch and arrival at the bottom
allows us to determine a descent time of 74 min to 5460 m. Dynamic
height calculations of the hydrographic data collected during the
cruise show a current at the OBS site in the upper 1000 m toward the
southeast, with very little motion below this depth. The maximum
velocity, 37 cm/sec, occurred at the surface. Assuming this upper-
bound velocity throughout the surface 1000-m layer, we arrive at a
deviation from launch position of 0.3 km to the southeast, corresponding
to a maximum error in epicentral travel time of 0.04 sec, which is

smaller than the OBS timing uncertainty.

Although the tape recorder jammed after only seven days, we can identify about 120 earthquakes during that period. Table 1 lists the P arrival time, S-P time, and P, S, and T amplitudes for these earthquakes.

The OBS records display a highly variable noise amplitude, probably connected with ocean current, which will be discussed later. The periods of high noise saturated the system so that detection of earthquakes was difficult during this time.

Figure 6 shows the S-P time distribution observed by the present OBS survey. Figure 6a includes all earthquakes, whereas Figure 6b includes only earthquakes with S-P times shorter than 37 sec. The observed earthquakes may be divided into three groups: (a) 19 $\leq$ S-P $\leq$ 24 sec, (b) S-P time $\sim$ 30 sec, and (c) S-P time $\sim$ 100 sec. From the U.S. Geological Survey Epicenter Determination Report (USGS-EDR), hypocenter determinations and land station data (A. Takagi, Tohoku University, Sendai, Japan, personal communication), we find that group (a) corresponds to aftershock activity of the 10 June (M = 7.0, Japan Meteorological Agency (JMA)) and the 13 June (M = 6.5, JMA), 1975 earthquakes and to earthquakes that occurred near the trench east of Sanriku, Japan. Group (b) epicenters cluster south of Erimo Peninsula on Hokkaido. Group (c) results from deep earthquakes that occurred along the seismic plane that dips under the Izu-Bonin Islands.

6

These three S-P groups account for most of the earthquakes observed by the OBS, but the remaining few show interesting features. In particular, on 14 August a microearthquake with 3.1 sec S-P time was recorded. If we assume an Omori coefficient of k = 6 km/sec, the distance between the OBS and the hypocenter becomes 18.6 km, suggesting that this earthquake occurred on the oceanic side of the Kuril Trench axis. Flexion of the sinking oceanic lithosphere, indicated by steps in the bottom topography near the trench [*Ludwig et al.*, 1966], probably causes such earthquakes. During the present survey we observed a low level of seismic activity near the bending lithosphere. This result is consistent with previous OBS observations [*Asada and Shimamura*, 1974] which show low seismicity on the oceanic side of the Kuril Trench. On the other hand, OBS observations on the oceanic side of the Japan Trench [*Nagumo and Kasahara*, 1976] yielded seismic activity six times greater than that of the continental slope, suggesting that the Kuril and Japan Trenches have different seismotectonic characteristics. In general, large, shallow focus earthquakes occur on the continental side of the trench and exhibit a thrust fault mechanism [*Kanamori*, 1971a]. However, the 1933 Sanriku earthquake (M = 8.3) showed a normal fault mechanism [*Kanamori*, 1971b], which is further evidence for different tectonic situations in the Kuril and Japan Trenches. One small event shows an S-P time of 5.5 sec (Figure 7b) and appears to have occurred at the trench axis.

Some earthquakes with S-P times of about 19-24 sec exhibit strong T-phases (see Figure 7). However, other tremors with about

30 sec S-P time are associated with lithospheric sinking beneath
Hokkaido and do not have a significant T-phase. Strong T-phase
source regions are located near the southwest and northeast boundaries
of the aftershock areas for the 10 June and 13 June earthquakes
and near the Japan Trench east of Sanriku, Japan. The aftershocks of
the 10 June and 13 June earthquakes occurred on the continental
slope, northwest of the Kuril Trench axis (Figure 8). To determine
the epicenters of the aftershocks, a "normal" focal depth of 35 km
was assumed (Japan, Hokkaido University, 1976). However, the present
survey recorded considerable T-phase activity from these aftershocks
and, since efficient T-phase generation is usually associated with
shallow focus, this activity implies that the foci were closer to the
surface than was assumed. Although the large magnitude earthquakes
in group (a) have generally large T-phases, two of these earthquakes
have relatively small T-phases while one tremor, with large P and S
wave amplitudes and S-P time of 19.8 sec, shows no T-phase energy
(Figure 9). These earthquakes probably occurred deeper than the
efficient T-phase generators.

The P waves appear to arrive 0.5 to 1.6 sec earlier on the
vertical than on the horizontal trace, as shown in Figure 7. This
time difference has also been reported for other OBS observations
[*Auld et al.*, 1969; *Hasegawa and Nagumo*, 1970; *Sutton et al.*, 1970].
Auld et al. hypothesized that this delay is caused by P to S wave
conversion at boundary layers one and two.

TRAVEL TIME ANOMALY IN THE SEISMIC ZONE

Utsu [1967] and *Oliver and Isacks* [1967] proposed a high velocity, high Q (HV, HQ) model of the seismic zone. *Utsu* [1967, 1971] estimated the seismic zone velocity to reach about 6% higher than that beneath Japan. *Mitronovas and Isacks* [1971] obtained 6-7% higher velocities than those for aseismic normal mantle near the Kermadec-Tonga region. Other investigators [*Katsumata*, 1960, 1970; *Hisamoto*, 1965; *Utsu and Okada*, 1968; *Kanamori and Abe*, 1968; *Jacob*, 1970; *Ishida*, 1970; *Nagamune*, 1971; *Yoshii*, 1972] obtained similar results. *Tada* [1972] and *Nagamune* [1973] estimated the absolute velocity in the descending slab and confirmed the above. *Nagumo et al.* [1970] used OBS data taken seaward of the Japan Trench and near the present OBS position to estimate the mean velocity in the slab. On the basis of hypocenter determinations by the Japan Meteorological Agency (JMA), they found that P and S velocities were 8% to 12% higher than those beneath the Japanese Islands.

It is well known that JMA hypocenters shows a symmetric shift from those of U.S. Coast and Geodetic Survey (USCGS) and the International Seismological Center (ISC) [*Utsu*, 1971; *Ichikawa*, 1976]. Their travel time tables also differ. JMA determines the best fit hypocenters from local stations. The Japanese data are strongly affected by a low or high velocity zone under Japan, and thus such hypocenter determinations may be shifted. Since hypocenter determinations from worldwide data appear less subject to these errors, we will use USGS parameters.

The hypocenters of seven earthquakes which we observed were determined by USGS (Table 2); their epicenters are shown in Figure 10. As discussed, most seismic activity arose from the Kuril, Hokkaido, and south Honshu regions. Although only one hypocenter was determined in the aftershock area of the 10 and 13 June earthquakes, many microearthquakes appear to have occurred in this region.

The present OBS station was just seaward of the Kuril Trench so that waves received from earthquakes occurring in the seismic zone and shallower than 300 km should have traveled entirely in the high-velocity layer (Figure 11a). An earthquake which occurs deeper than 300 km may have a travel path outside of the seismic zone (Figure 11b). The P travel time and S-P time relation (Figure 12) show that OBS arrivals have slightly higher V_p/V_s ratios (about 1.795) than the usual upper mantle value (1.77, corresponding to Poisson's ratio, $\sigma = 0.265$) [Utsu, 1969; Nagumo et al., 1970; Nagamune, 1973]. Figure 13 shows the relation of P arrival to S-P time for each earthquake. Note that the OBS and land station arrivals fall on the same V_p/S_s line.

Nevertheless, travel time curves (Figure 14) for five earthquakes show significant OBS travel time anomalies (-3.3 to -10.6 sec, or -6.6% to -16.4% of the travel time for P; and -4.6 to -17.6 sec, or -5.1% to -13.1% of the travel time for S) from the Jeffreys-Bullen travel time curves (Table 3). Two earthquakes, however, have nearly normal P and S arrival times, as indicated by the Jeffreys-Bullen (J-B) travel time curves (Figure 15). Both of

these earthquakes had nearly the same location and depth, south of Honshu and 390 km deep. For the four remaining earthquakes with focus deeper than 50 km, average velocities over the path range from 8.58 to 8.86 km/sec ($\overline{V}_p$) and 4.79 to 4.87 km/sec ($\overline{V}_s$). The shallow focus earthquake which occurred in the aftershock area discussed above yielded average velocities of 7.85 km/sec for P waves and 4.36 km/sec for S waves.

The large travel time anomalies and their associated average velocities can be interpreted by a high velocity (HV) model for the descending lithosphere. It appears that wave paths for the anomalous arrivals are within the HV layer, while normal arrivals travel through the low velocity (LV) layer beneath the oceanic lithosphere.

Ludwig et al. [1966] and *Den et al.* [1971] determined the crustal section across the Japan and Kuril Trenches, respectively, and found their structures to be similar. We will assume the composite profile shown in Figure 16 using their results and compute the upper mantle velocity (assumed constant) for individual earthquakes. The results are also listed in Table 3.

The uppermost layer of the dipping slab displays typical oceanic mantle P velocity (8.12 km/sec), as revealed by the only shallow earthquake, whereas the deeper section shows very high P velocity, ranging between 8.65 and 8.97 km/sec, as indicated by earthquakes with foci between 50 and 230 km. Assuming $V_p/V_s = 1.795$, we can estimate the corresponding shear velocities as 4.52 km/sec for the upper part of

the slab and 4.80 km/sec averaged over the upper 230 km. This value
of shear velocity in the top of the descending slab agrees with other
estimates for the upper mantle [*Abe and Kanamori*, 1970], but our
shear velocity estimate for the slab between 50- and 230-km depth is
0.2 to 0.3 km/sec higher than that for normal oceanic mantle. Note
that the two nearby earthquakes with normal arrival times yield about
8.45 km/sec for compressional waves and 4.70 km/sec for shear waves.
Assuming the Jeffreys-Bullen velocity structure below the Mohorovicic'
discontinuity and the oceanic crustal structure as before (see
Figure 16), the mean mantle compressional wave velocity becomes 8.70
km/sec. The earthquakes with normal arrivals indicate about 3% lower
velocity in the upper 390 km of the oceanic mantle (see Figure 11b).
This velocity decrease in the deep mantle is consistent with the LV
models of *Utsu* [1967] and *Oliver and Isacks* [1967]. If the LV layer
is 100 km thick, it would imply a 12% velocity decrease in this layer.

Since JMA hypocenter determinations and origin times differ
considerably from those of USGS, especially for deep earthquakes, we
have calculated average velocities for five earthquakes on the basis
of JMA data. Table 2 shows the JMA parameters for these earthquakes
and Table 3 compares the corresponding average velocities. We see
that the results based on JMA data do not significantly alter the
velocities calculated from USGS data; earthquakes which implied high
velocity in the dipping slab again result in high velocity, while
earthquakes with normal arrivals again yield a low velocity beneath
the oceanic lithosphere.

Table 2 lists the errors in origin time, depth, and location for USGS hypocenter parameters used in the present analysis. The hypocenter of the 14 August earthquake off the east coast of Honshu was well determined; moreover, the USGS and JMA determinations both yield high average velocities. The USGS error accounts for about $\pm$ 0.05 km/sec uncertainty. As mentioned earlier, the OBS positioning error is negligible and the clock error is about $\pm$ 0.1 sec. Considering the hypocenter parameter errors for the other earthquakes with early arrivals results in a lower limit for the averaged mantle P velocity of 8.5 km/sec and S velocity of 4.8 km/sec in the descending slab. A similar analysis using the earthquakes with normal arrivals results in an upper limit for mantle P velocity of 8.4 km/sec, and for mantle S velocity of 4.7 km/sec averaged over the upper 390 km.

The present value of velocity in the descending slab is 0.2 to 0.4 km/sec higher than previous estimates [*Nagumo et al.*, 1970; *Nagamune*, 1973] which agree with results for old oceanic mantle. These lower velocity estimates may be due partly to poor hypocenter determinations or to the use of data from land stations which include LV paths. The method used in the present analysis is very sensitive to the accuracy of hypocenter determination. To confirm our results we plan further independent observations involving an OBS array along the trench to calculate the apparent velocity.

Q STRUCTURE

Using the playback scheme shown in Figure 5, we generated a set of sonograms which show the spectrum as a function of time for various earthquakes. Figure 17 shows some examples of sonograms in which the contours represent 6-dB increments in amplitude. The earthquake with an S-P time of 100.9 sec (Figure 17a) has a relatively stronger high-frequency component than the earthquake with 19.2 sec S-P time (Figure 17b). The noise with dominant frequencies of 3.3 and 9.9 Hz appears to be excited by earthquakes.

Figure 18 shows some examples of corrected spectra derived as a cut in time through sonogram records. If we assume a flat source spectrum for velocity amplitude [*Asada and Takano*, 1965; *Asada and Shimamura*, 1976], we can estimate minimum Q values. Figure 19 illustrates the observed slopes for selected earthquakes, with slopes corresponding to various Q values shown in the same figure. Earthquakes with S-P times longer than 43 sec yield a Qs (Q for S waves) between 4000 and 6000. On the other hand, earthquakes with shorter S-P times than 43 sec indicate a Qs of 1000 to 1500. Qs values for earthquakes with S-P times between 19 and 24 sec cluster in a narrow region. Although most of the Q values are obtained for S waves because of the generally low amplitude of P waves, three Qp (Q for P waves) values were determined. Earthquakes with S-P times of about 25 sec have a Qp between 600 and 850, while one earthquake with an S-P time of 70 sec shows Qp ∿ 3000 and Qs ∿ 4000.

The high Qs ($\sim$ 5000) obtained for long-distance earthquakes suggests an unusual Q mechanism, such as an upper mantle wave guide with low attenuation of the high-frequency component [*Shurbet*, 1962, 1964; *Walker and Sutton*, 1971; *Sutton and Walker*, 1972].

Earthquakes studied here have paths in the dipping slab or in the top of the oceanic lithosphere, so the Q obtained might reflect the Q of the dipping slab.

A Qs value of 1000 to 1500 is higher than the typical Qs ($\sim$ 150) for the Japanese Archipelago [see for example, *Nakashima et al.*, 1976]. A typical Qp value for the upper mantle is about 2000 [*Fraiser and Filson*, 1972]. If Qp/Qs $\sim$ 9/4 [*Nakashima et al.*, 1976], the present result is consistent with previous results. The present result for long-distance earthquakes is similar to that obtained by *Asada and Shimamura* [1976]. Although *Oliver and Isacks* [1967] assumed a flat displacement source mechanism, they obtained Qs $\sim$ 1000 in the dipping slab, which is consistent with our result.

We have also calculated Q using a different set of assumptions. If we assume identical source spectra and identical attenuation mechanisms for all earthquakes, we find Qs $\sim$ 5000, deduced from the change in amplitude with distance for a pair of earthquakes. Although the above assumption is more reasonable than that of a flat source spectrum for velocity displacement, the Q value thus obtained is strongly affected by the amplitude decay with frequency for the particular two earthquakes. A future long-duration experiment or array measurement may allow us to use this alternate method effectively.

OBS NOISE

The seven-day OBS record is characterized by a nonstationary noise background which often saturated the recording system (1000 µcm/sec, peak-to-peak) so that only the largest earthquakes could be detected, but which contained two windows of one day and one-half day during which the noise level was about 10 µcm/sec, peak-to-peak. These two quiet periods include most of the detected earthquakes listed in Table 1.

Throughout the recording the noise spectrum was strongly peaked about 3.3 Hz, with a secondary peak near 9.9 Hz, as shown in Figure 17. Earthquake arrivals enhance this noise which is superimposed on the earthquake spectrum, implying that at these frequencies the earthquake somehow excites resonance, either connected with the OBS system, the crustal structure, or some combination thereof. Previous OBS observations in the North Atlantic using the same seismometer and housing exhibit a resonance near 8 Hz, which suggests that the OBS system alone cannot account for the present noise character.

Sutton et al. [1965] found a correlation of microseism activity with wave height, which led us to examine the daily weather maps for the Hokkaido region during the week of recording. Ship reports of wind, wind wave amplitude, and swell amplitude from 35° to 45°N and 140° to 160°E were averaged for each day from 11 to 18 August. However, wind, wave, and swell records were featureless during this time and show no obvious correlation with the observed seismic noise amplitude.

A careful examination of the noise amplitude in time reveals an indication of semidiurnal periodicity, but the level frequently is either saturated with noise or so quiet that we cannot detect any modulation. A 12-hour periodicity suggests tidal currents as a noise source. Bottom pressure recorder P8 was located within 3 km of the OBS and thus recorded the pressure fluctuation due to passage of the tide at that site. We find little correlation of the OBS noise amplitude with this pressure data. However, this is not surprising, since bottom currents are often dominated by internal modes, which are not phase-locked with the barotropic tide.

Bradner et al. [1965a] suggested Kármán vortices around the radio antenna as a source of observed noise spectral peaks around 2 Hz. In a study of microseism sources in the Pacific Basin [*Bradner et al.,* 1965b], they often found peaks in background spectra between 2 and 4 Hz which remain unexplained. Unfortunately, the records were limited to about one-hour duration so any possible fluctuation with tidal frequency could not be detected.

The present OBS system has been designed with insufficient regard for interaction with bottom currents. Future instruments will be reconfigured to present a smaller cross section to water currents, will rest on a wide, three-point base, and will employ a low-profile antenna. In addition, we plan to deploy a bottom current meter nearby for direct comparison.

CONCLUSIONS

A single pop-up OBS was deployed east of Hokkaido, Japan, on the oceanic side of the Kuril Trench in August 1975. One hundred twenty earthquakes were observed during the seven-day record, which included five noisy days.

The hypocenters of seven earthquakes were determined by USGS, and five of these were also determined by JMA. Five earthquakes had wave paths in the seismic zone dipping under the Kuril Trench, an area which is generally characterized by high velocity and high Q. Two of the earthquakes had wave paths in the LV, LQ zone beneath the Pacific oceanic lithosphere.

The travel times for the five earthquakes which had paths in the dipping slab show anomalously early arrivals compared with J-B travel time curves. Travel time anomalies for P and S waves are distributed between -3.3 and -10.6 sec (or -6.6% and -16.4%) and between -4.6 and -17.4 sec (-5.1% and -13.1%), respectively. On the other hand, the two earthquakes whose paths were in the LV, LQ zone beneath the oceanic lithosphere show nearly normal arrival times. Assuming an oceanic crustal structure based on *Ludwig et al.* [1966] and *Den et al.* [1971], the average mantle velocity was calculated. The resulting compressional velocity in the dipping slab is higher than 8.5 km/sec below 50-km depth. This value is 0.2-0.4 km/sec higher than previous estimates. The shear velocity in the dipping slab is approximately 4.8 km/sec. Although these velocities are consistent with those of periodotite [*Kasahara et al.*, 1968a, 1968b], it is

18

difficult to explain the velocity difference between oceanic mantle and dipping lithosphere, if both lithospheres have the same rock composition.

Examination of the effects due to different hypocenter parameters applied (USGS or JMA) does not change the above conclusions.

The Q analysis revealed $1000 < Q_s < 1500$ in the dipping slab and $4000 < Q_s < 6000$ for earthquakes with S-P times greater than 43 sec. These values suggest high Q in the dipping slab and a wave propagation mechanism such as channel waves that exhibit relatively low attenuation for high frequencies.

The noise level varied during the OBS observations. The noise has peak frequencies at 3.3 Hz and 9.9 Hz. The noise variation with time shows a weak correlation with bottom currents.

REFERENCES

Abe, K. and H. Kanamori. 1970. Upper mantle structure of the Philippine Sea in island arc and ocean, p. 85-91 in M. Hoshino and H. Aoki (eds.), Tokai University Press, Tokyo.

Asada, T. and H. Shimamura. 1974. The ocean bottom seismometer as a new tool for geophysics, *Kagaku, 44,* 278-285. [In Japanese]

Asada, T. and H. Shimamura. 1976. Observation of earthquakes and explosions at the bottom of the western Pacific: Structure of oceanic lithosphere revealed by Longshot experiment, p. 135-153 in G. H. Sutton, M. H. Manghnani, and R. Moberly (eds.), *The Geophysics of the Pacific Ocean Basin and Its Margin: A Volume in Honor of George P. Woollard, Geophys. Monogr. Ser., 19, Am. Geophys. Union,* Washington, D.C.

Asada, T. and K. Takano. 1965. Attenuation of short period P waves in the mantle, *J. Phys. Earth, 11,* 25-34.

Auld, B., G. Latham, A. Nowroozi, and L. Seeber. 1969. Seismicity off the coast of northern California determined from ocean bottom seismic measurements, *Bull. Seismol. Soc. Am., 59,* 2001-2015.

Bradner, H., J. Dodds, and R. Foulks. 1965a. Coherence measurements with time sampling ocean-bottom seismometers, *Proc., IEEE, 53,* 1906-1908.

Bradner, H., J. G. Dodds, and R. E. Foulks. 1965b. Investigation of microseism sources with ocean-bottom seismometers, *Geophysics, 30,* 511-526.

20

Den, N., H. Hotta, S. Asano, T. Yoshii, N. Sakajiri, and Y. Ichinose.
1971. Seismic refraction and reflection measurements around
Hokkaido, Part 1, Crustal structure of the continental slope off
Tokachi, *J. Phys. Earth*, *19*, 329-345.

Efimov, V. V., Robert R. Harvey, Sergei S. Lappo, Gaylord R. Miller,
and Sergei L. Soloviev, Edge Waves in the Kuril-Hokkaido
Region, *J. Phys. Ocean.*, in press.

Fraiser, C. W. and J. Filson. 1972. A direction measurement of the
earth's short period attenuation along a teleseismic ray path,
J. Geophys. Res., *77*, 3782-3787.

Hasegawa, S. and S. Nagumo. 1970. Construction of a long life magnetic
tape recorder and some features of ocean-bottom seismograms,
Bull. Earthquake Res. Inst., Univ. Tokyo, *48*, 967-981. [In
Japanese with English abstract]

Hisamoto, S. 1965. On the anomaly of travel time of S waves observed in
eastern Japan, *J. Seismol. Soc. Japan*, *18*, Part 1, 142-153, Part 2,
195-203. [In Japanese with English abstract]

Ichikawa, S. 1976. Hypocenter determination of south Kuril earthquakes,
Abstract from 1976 spring meeting, *Seismol. Soc. Japan*. [In Japanese]

Ishida, M. 1970. Seismicity and travel time anomaly in and around Japan,
Bull. Earthquake Res. Inst., Univ. Tokyo, *48*, 1023-1051.

Jacob, K.H. 1970. Three dimensional seismic ray tracing in a laterally
heterogeneous spherical earth, *J. Geophys. Res.*, *75*, 6673-6689.

Japan. Hokkaido University. 1976. Observation of the earthquake of June 1975 in the east off Hokkaido, Report of the Coordinating Committee on Earthquake Prediction, 15, 6-7. [In Japanese]

Japan Meteorological Agency, Seismic Activity Measurement Center. 1976. The earthquake off eastern part of Hokkaido, June 1975, Report of the Coordinating Committee on Earthquake Prediction, 15, 8-10. [In Japanese]

Kanamori, H. 1971a. Great earthquakes at island arc and the lithosphere, *Tectonophysics, 12*, 187-198.

Kanamori, H. 1971b. Seismological evidence for a lithospheric normal faulting, the Sanriku earthquake of 1933, *Phys. Earth Planet. Inter., 4*, 289-300.

Kanamori, H. and K. Abe. 1968. Deep structure of island arcs as revealed by surface waves, *Bull. Earthquake Res. Inst., Univ. Tokyo, 46*, 1001-1025.

Kasahara, J., I. Suzuki, M. Kumazawa, Y. Kobayashi, and K. Iida. 1968a. Anisotropism of P-wave in Dunite, *J. Seismol. Soc. Japan, 21*, 222-228. [In Japanese with English abstract]

Kasahara, J., I. Suzuki, M. Kumazawa, and K. Iida. 1968b. Anisotropism of S-wave in Dunite, *J. Seismol. Soc. Japan, 21*, 229-236. [In Japanese with English abstract]

Kasahara, J., T. Ouchi, M. Yanagisawa, and S. Nagumo. 1973. Low-power digital coding digital display crystal clock and timer utilizing C-Mos IC, *J. Seismol. Soc. Japan, 26*, 294-300, 1973. [In Japanese]

22

Kasahara, J., S. Koresawa, T. Ouchi, and S. Nagumo. 1974a. Free-fall pop-up ocean bottom seismograph system, *Earthquake Res. Inst., Univ. of Tokyo, Spec. Bull. 13*, 1-16. [In Japanese with English abstract]

Kasahara, J., S. Nagumo, S. Koresawa, and T. Ouchi. 1974b. Low power amplifier and tape recorder for the ocean bottom seismograph, *J. Seismol. Soc. Japan, 27*, 75-77. [In Japanese]

Katsumata, M. 1960. The effect of seismic zone upon the transmission of seismic waves, *Kenshinjiho (Quart. J. Seismol.), 25*, 89-95. [In Japanese]

Katsumata, M. 1970. Seismicity and some related problems in and near the Japanese islands, *Kenshinjiho (Quart. J. Seismol.), 35*, 75-142. [In Japanese]

Ludwig, W. J., J. I. Ewing, M. Ewing, S. Murauchi, N. Den, S. Asano, H. Hotta, M. Hayakawa, T. Asanuma, K. Ichikawa, and I. Noguchi. 1966. Sediments and structure of the Japan trench, *J. Geophys. Res., 71*, 2121-2137.

Mitronovas, W. and B. L. Isacks. 1971. Seismic velocity anomalies in the upper mantle beneath the Tonga-Kermadec island arc, *J. Geophys. Res., 76*, 7154-7180.

Nagamune, T. 1971. Seismic waves associated with the anomalous zone in the upper mantle, *Geophys. Mag., 35*, 123-135.

Nagamune, T. 1973. Seismic wave velocities in the deep earthquake zone, *Pap. Meteorol. Geophys., 24*, 139-156. [In Japanese with English abstract]

Nagumo, S. and J. Kasahara. 1976. Ocean-bottom seismograph study of the western margin of the Pacific, p. 155-167 in G. H. Sutton, M. H. Manghnani, and R. Moberly (eds), *The Geophysics of the Pacific Ocean Basin and Its Margin: A Volume in Honor of George P. Woollard, Geophys. Monogr. Ser., 19, Am. Geophys. Union*, Washington, D. C.

Nagumo, S., S. Hasegawa, S. Koresawa, and H. Kobayashi. 1970. Ocean-bottom seismographic observation at the offside of Japan trench near the Erimo seamount, *Bull. Earthquake Res. Inst., Univ. of Tokyo, 48*, 769-792.

Nakashima, T., T. Moriya, and H. Okada. 1976. Q distribution in Hokkaido, estimated by the S/P method, abstract from 1976 spring meeting, *Seismol. Soc. Japan*. [In Japanese]

Oliver, J. and B. Isacks. 1967. Deep earthquake zones, anomalous structures in the upper mantle, and the lithosphere, *J. Geophys. Res., 72*, 4259-4275.

Shurbet, D. H. 1962. High frequency P and S phases, *Bull. Seismol. Soc. Am., 52*, 957-962.

Shurbet, D. H. 1964. The high-frequency S phase and structure of the upper mantle, *J. Geophys. Res., 69*, 2065-2070.

Soloviev, S. L., Miller, G. R., *et al*. 1976. Preliminary Results of the First Soviet-American Tsunami Expedition, *HIG-76-8, Hawaii Inst. Geophys., Univ. Hawaii*, Honolulu, 71 p., in press.

Sutton, G. H. and D. A. Walker. 1972. Oceanic mantle phases recorded on seismographs in the Northwestern Pacific at distances between 7° and 40°, *Bull. Seismol. Soc. Am., 62*, 631-655.

24

Sutton, G. H., W. G. Mcdonald, D. D. Prentiss, and S. N. Thanos. 1965. Ocean-bottom seismic observatories, *Proc. IEEE*, *53*, 1909-1921.

Sutton, G. H., M. E. Odegard, N. Mark, and N. J. LeTourneau. 1970. Research in seismology related to the Columbia ocean-bottom seismograph, *HIG-70-12, Hawaii Inst. Geophys.*, Univ. Hawaii, Honolulu, 66 p.

Tada, T. 1972. P wave velocity distribution in the down-going slab, *J. Seismol. Soc. Japan*, *25*, 310-317. [In Japanese with English abstract]

Utsu, T. 1967. Anomalies in a seismic wave velocity and attenuation associated with a deep earthquake zone (I), *J. Fac. Sci., Univ. Hokkaido Ser. 7: Geophysics 3*, 1-25.

Utsu, T. 1969. Ratio of V_p/V_s in the upper mantle beneath the island arcs of Japan, *J. Seismol. Soc. Japan*, *22*, 41-53. [In Japanese with English abstract]

Utsu, T. 1971. Seismological evidences for anomalous structure of island arc with special reference to the Japanese region, *Rev. Geophys. Space Phys.*, *9*, 839-890.

Utsu, T. and H. Okada. 1968. Anomalies in seismic wave velocity and attenuation associated with a deep earthquake zone (III), *J. Fac. Sci., Univ. Hokkaido, Ser. 7: Geophysics, 3*, 65-84.

Walker, D. A. and G. H. Sutton. 1971. Oceanic mantle phases recorded on hydrophones in the North-western Pacific at distances between 9° and 40°, *Bull. Seismol. Soc. Am.*, *61*, 65-78.

Yoshii, T. 1972. Features of the upper mantle around Japan inferred from gravity anomalies, *J. Phys. Earth*, *20*, 23-24.

TABLES

Table 1. Arrival times, S-P times and amplitudes of P, S, and T phases for OBS observations during the 1975 Soviet-American Tsunami Expedition. Amplitudes are taken from the vertical, low gain channel.

Month	Day	Hour	Minute	Second Phase	Second	S-P sec	Phase	A_P mm	A_S mm	A_T mm	Comments
8	11	08	26	IP	56.6	28.4	IS	0.8	10		
		08	31		40.8		IS	--	6		
		09	13	EX	20.1	13.3	ES	--	5		
		12	05	EP	31.7	24.7	IS	--	7		
		13	50	EP	04.5	22.9	ES	1.5	6		
		14	57	IP	16.5	3.1	ES	2.5	14		
		15	31		52.3		IS	--	10		
		16	32	EP	00.4			5			
				EX	09.9			6			
				EX	32.4			5			
				EX	37.7			Sat.			
		20	01	EP	14.0	29.9	IS	2	7		
		21	28	EP	29.9	30.0	IS	6	Sat.		
		22	42	EP	06.2	31.0	ES	1	2		
		23	16		49.4		IS	--	5		
	12	01	54		40.8		ES	--	5		
		02	01		54.2		ES	--	10		
		02	09	EX	50.7			--			
		03	57		17.8		ES	--	4		
		04	07		49.4		ES	--	3		
		07	07		52.3		ES	--	3		
					53.5		ES	--	40		
		08	54	EP	20.8	122.0	ES	--	40		

SOUTH OF HONSHU, JAPAN
$m_b = 4.6$

Table 1 (continued)

Month	Day	Hour	Minute	Second	Phase	S-P sec	Phase	A_P mm	A_S mm	A_T mm	Comments
8	12	12	54	41.3	EP	52.3	IS	7	Sat.		KURIL ISLANDS, Mb = 3.9
		14	03	24.5	IP	19.8	IS	6	Sat.		
		14	23	45.1	EP	123.6	ES	Sat.	Sat.		SOUTH OF HONSHU, JAPAN Mb = 5.7
		14	25	13.6	EP			Sat.	--		
		17	33	13.0			IS	--	16		
		21	12	19.7			ES	--	3		
		22	15	15.9	IP	69.5	IS	2	7		
		23	05	44.5	EP	100.8	IS	--	3		
		23	36	19.2	EP	74.3	IS	1	3		
	13	00	05	01.0	EP	59.6	IS	--	4		
		01	58	30.1			IS	--	1		
		02	09	27.1			IS	--	1.5		
		02	28	25.9			IS	--	1.5		
		02	53	59.3	IP	36.2	IS	1	3		
		03	23	31.0	EP	20.4	IS	1	6	1	
		04	16	29.4	EP	84.0	IS	2	7		
		05	05	23.2	EP	28.7	ES	0.5	1.5		
		05	15	09.6	EP	20.4	IS	--	4		
		05	28	06.3	IP	25.4	IS	1	4		
		07	01	01.0			IS	--	2		
		09	05	52.1	EP	21.2	ES	--	1.5		

Table 1 (continued)

Month	Day	Hour	Minute	Second Phase	S–P sec	Phase	A_P mm	A_S mm	A_T mm	Comments
8	13	09	28	IP 03.9	5.5	IS	2	6		
		10	12	EP 37.6	57.9	IS	1	11		
		11	15	EP 54.3	32.6	IS	--	1.5		
		11	20	IP 54.9	{ 17.6 / 32.2 }	ES / IS	1	2 / 5		
		12	02	06.7		IS	--	1.5		
		12	58	IP 32.3	23.0	IS	6	35	2	
		13	24	EP 12.1	19.3	IS	0.5	1		
		13	40	IP 11.6	21.3	IS	2	6		
		13	53	IP 22.1	22.9	IS	13	Sat.	25	KURIL ISLANDS, Mb = 4.8
		14	31	IP 34.6	25.0	IS	2	22		
		14	52	39.6		ES	--	3		
		15	12	36.2		IS	--	3		
		15	27	11.7		IS	--	3	2	
		16	11	07.2		IS	--	3		
		16	14	{ IP 11.0 / EP 16.6 }	33.3	IS	35	Sat.		HOKKAIDO, JAPAN, Mb = 4.3
		17	11	49.5		IS	--	7		
		19	36	IP 09.6	32.7	IS	1	1.5		
		20	47	EP 01.7	90.2	ES	1	1.5		
		20	52	IP 36.8	90.7	IS	3	6		OFF E. COAST HONSHU, JAPAN Mb = 4.0 (33°N, 143°E, OT = 20H50M41S)
		21	01	EP 45.8	24.7	ES	--	0.5		

Table 1 (continued)

Month	Day	Hour	Minute	Second	Phase	S-P sec	Phase	A_P mm	A_S mm	A_T mm	Comments
8	13	21	09	55.9	EP	24.2	IS	0.5	3		
		22	13	18.0	EP	21.9	IS	--	3		
		22	23	18.4	IP	43.7	IS	8	11		
		22	40	05.9	EP	47.9	IS	--	3		
		23	14	54.9			IS		2		
		23	20	24.5	IP	23.9	ES	2	8	2	
		23	38	01.7	EP	16.4	IS	0.5	6		
		23	43	07.0	IP			2.5	--		
		23	44	05.2	EX			6	--		
		23	45	25.3	EX			3	--		
8	14	00	04	04.4			IS	--	3		
		07	36	41.8			ES	--	5	2(?)	
		09	59	59.2	EP	33.6	IS	2	7		
		10	36	43.5			ES	--	1		
		11	04	49.1	EP	28.7	ES	--	--		
		13	02	35.7	EP	19.6	ES	--	2		
		18	10	45.8	EP	61.8	ES	--	Sat.		
	15	03	12	15.9	EP	28.0	ES	--	Sat.		
		04	30	00.2			ES	--	--		
		20	22	35.8	EP	23.1	ES	--	1.5		
		21	57	22.4			IS	--	2		
		23	09	05.8	EP	65.3	IS	--	2		
		23	10	48.2	EX			1			
		23	35	06.5	EP	43.3	IS	1	3		NEAR E. COAST OF HONSHU, JAPAN, Mb = 5.5

Table 1 (continued)

Month	Day	Hour	Minute	Second	Phase	S-P sec	Phase	A_P mm	A_S mm	A_I mm	Comments
8	16	00	25	43.4	IP	20.4	IS	2.5	34	2	
		00	39	41.4	IP	17.7	IS	--	4		
		01	53	57.1	EP	20.1	IS	--	2.5		
		02	19	19.4	EP	21.9	IS	1	4		
		02	45	53.0	IP	100.9	IS	3	12		SOUTH OF HONSHU, JAPAN Mb = 4.7
		03	21	35.2	EP	21.7	IS	1	2		
		03	25	48.5	EP	93.5 }					
				51.2	IP	90.8	IS	1	5		
		04	24	51.8	EP	29.1	IS	1	5		
		04	27	35.0			IS	--	1		
		05	11	07.8	EP	34.9	IS	--	6		
		06	21	24.8			IS	--	4		
		08	00	01.5			ES	--	9		
		08	46	30.8			ES	--	16		
		12	36	30.3			IS	--	15		
		19	19	41.8	EP	41.7	ES	--	Sat.		
	17	00	38	07.9			ES	--	Sat.		
		02	48	37.4			ES	--	6		
		02	59	05.5	EP	14.7 }	IS	7	Sat.		
				07.1	EP	13.1 }		7			
		08	13	52.5			ES		4		
		13	51	14.0	EP	34.3	ES	--	3		
		14	04	26.1	IP	31.8	IS	8	Sat.		

Table 1 (continued)

Month	Day	Hour	Minute	Second	Phase	S-P sec	Phase	AP mm	AS mm	AT mm	Comments
8	17	14	53	47.2	EP	18.0	IS	1.5	4		
		14	57	02.5			IS	--	3		
		15	16	57.9			IS	--	7		
		18	17	05.9	EP	28.9	IS	2	7		
		20	04	47.5	EP	19.1	IS	3	6		
		21	05	33.8			IS	--	7		
		23	17	{16.4	EP	72.7	IS	3	10		
				17.8	EP	71.3	IS	3			
		2:	59	41.6	EP	22.8	IS	3	8	3	
	18	01	51	16.6	IP	19.2	IS	3	10	5	
		02	08	56.0			ES	--	1.5		
		02	11	32.4	EP	48.0	IS	0.5	16		
		02	47	16.9	EP	15.5	IS	0.5	1.5		
		02	49	55.8	IP	25.2	IS	7	Sat.		

HOKKAIDO, JAPAN
Mb = 3.8 (42°N, 143°E,
OT = 02H49M22S)

Table 2. Hypocenter parameters for the seven earthquakes used in the present analysis, determined from U.S. Geological Survey and Japan Meteorological Agency data. Japan Meteorological Agency data are in parentheses.

Date	Origin Time Hour	Min	Second	Latitude	Longitude	Depth km	Body wave magnitude M_b	Region	No. of stations	Standard deviation seconds
Aug. 12	08	51	41.3 ± 0.25 (40.8 ± 0.40)	31.971°N ± 3.35 km (31.867°N ± 3.67 km)	138.097°E ± 2.68 km (138.333°E ± 4.65 km)	385.1 ± 1.9 (380)	4.6 (5.7)	South of Honshu, Japan	77	0.8
Aug. 12	12	53	37.4 ± 1.02	45.726°N ± 7.87 km	149.722°E ± 5.21 km	137.4 ± 12.8	3.9	Kuril Islands	7	0.4
Aug. 12	14	21	4.7 ± 0.17 (4.9 ± 0.3)	32.042°N ± 1.72 km (31.950°N ± 3.67 km)	137.715°E ± 1.75 km (138.200°E ± 1.58 km)	390.8 ± 1.6 (400)	5.7 (6.9)	South of Honshu, Japan	245	1.0
Aug. 13	13	52	53.2 ± 0.41	43.060°N ± 4.30 km	147.982°E ± 5.66 km	[1]33	4.8	Kuril Islands	21	0.9
Aug. 13	16	13	28.5 ± 0.35 (29.9 ± 0.2)	41.683°N ± 3.36 km (41.750°N ± 1.89 km)	142.144°E ± 7.34 km (142.083°E ± 2.77 km)	76.2 ± 4.6 (70)	4.3 (4.1)	Hokkaido, Japan	12	1.0
Aug. 14	18	9	27.6 ± 0.10 (28.3 ± 0.2)	37.103°N ± 2.07 km (37.067°N ± 0.60 km)	141.007°E ± 2.43 km (141.133°E ± 1.53 km)	52.0 (50)	5.5 (5.5)	Near east coast of Honshu, Japan	113	0.9
Aug. 16	2	43	49.0 ± 0.28 (48.8 ± 0.2)	34.120°N ± 3.80 km (34.183°N ± 3.67 km)	138.771°E ± 4.09 km (138.900°E ± 3.04 km)	231.5 ± 2.3 (240)	4.7 (4.7)	Near south coast of Honshu, Japan	37	1.0

[1]Normal depth assumed by U.S. Geological Survey.

Table 3. Summary of results for the seven earthquakes used in the present analysis. Origin times and focal depths are from the U. S. Geological Survey Epicenter Determination Record

Origin time Date	hour	min	sec.	Epicentral distance km	Focal depth km	Region	Travel time Anomalies ΔP per-cent sec.		ΔS per-cent sec.		Average velocity[1] $\bar{V}_P$ km/sec	$\bar{V}_S$ km/sec	Mantle velocity[2] V_P km/sec	V_S km/sec
Aug. 12	08	51	41.3	1283.2	385.1	South of Honshu, Japan	+2.4	+1.5	0.0	0.0	8.40 (8.35)	4.76 (4.74)	8.44 ±0.05	4.70 ±0.03
Aug. 12	12	53	37.4	549.3	137.4	Kuril Islands	-9.6	-13.1	-14.0	-10.8	8.86	4.87	8.97 +0.34	5.00 ±0.19
Aug. 12	14	21	04.7	1296.6	390.8	South of Honshu, Japan	+2.0	+1.3	-0.3	-0.1	8.44 (8.37)	4.77 (4.73)	8.48 ±0.03	4.72 ±0.02
Aug. 13	13	52	53.2	223.5	[3]33	Kuril Islands	-3.3	-10.2	-4.6	-8.2	7.85	4.36	8.12 ±0.28	4.52 ±0.16
Aug. 13	16	13	28.5	356.5	76.2	Hokkaido, Japan	-7.0	-16.4	-11.4	-13.1	8.58 (8.91)	4.83 (4.96)	8.75 ±0.29	4.87 ±0.16
Aug. 14	18	09	27.6	668.6	52.0	Near east coast of Japan	-10.6	-12.0	-17.4	-11.1	8.58 (8.62)	4.79 (4.79)	8.65 ±0.05	4.82 ±0.03
Aug. 16	02	43	49.0	1051.7	231.5	South of Honshu, Japan	-8.8	-6.6	-12.0	-5.1	8.68 (8.59)	4.79 (4.74)	8.74 ±0.07	4.87 ±0.04

[1]Travel time (straight distance) between focus and OBS, calculated for U.S. Geological Survey hypocenter parameters. Parentheses apply to Japan Meteorological Agency hypocenter parameters.

[2]Assuming constant mantle velocity and crustal structure shown in Figure 16. $V_S = V_P/1.795$. Errors were determined using the errors reported with U.S. Geological Survey hypocenter parameters.

[3]Normal depth assumed by U.S. Geological Survey.

FIGURES
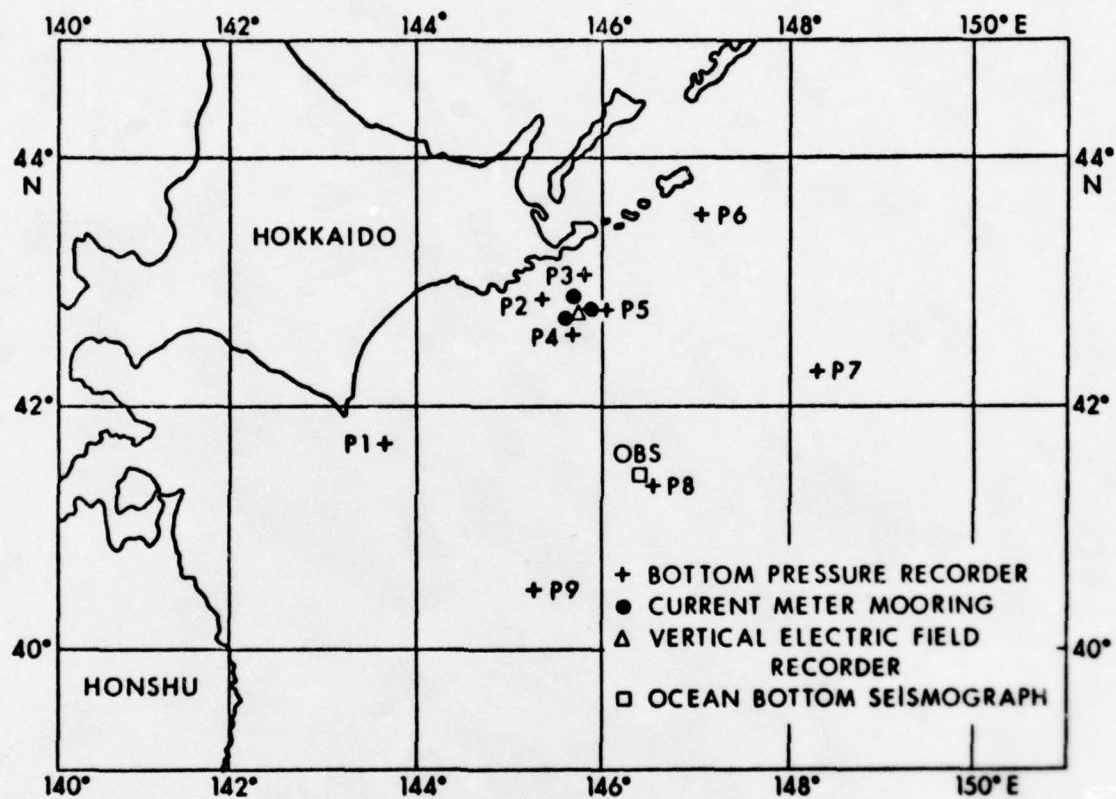
Fig. 1. Instrument locations during the 1975 Soviet-American Tsunami Expedition.
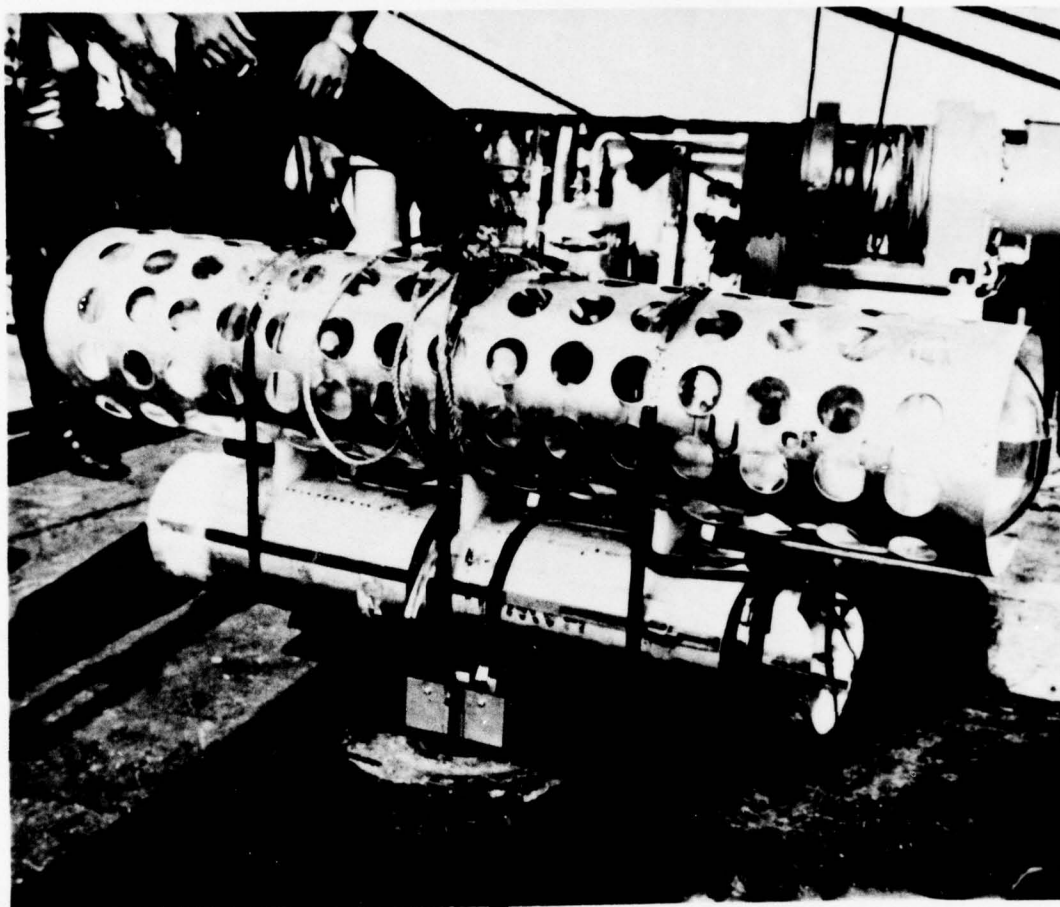
Fig. 2. Pop-up ocean bottom seismograph on board the Soviet vessel R. V. *Valerian Uryvaev*.
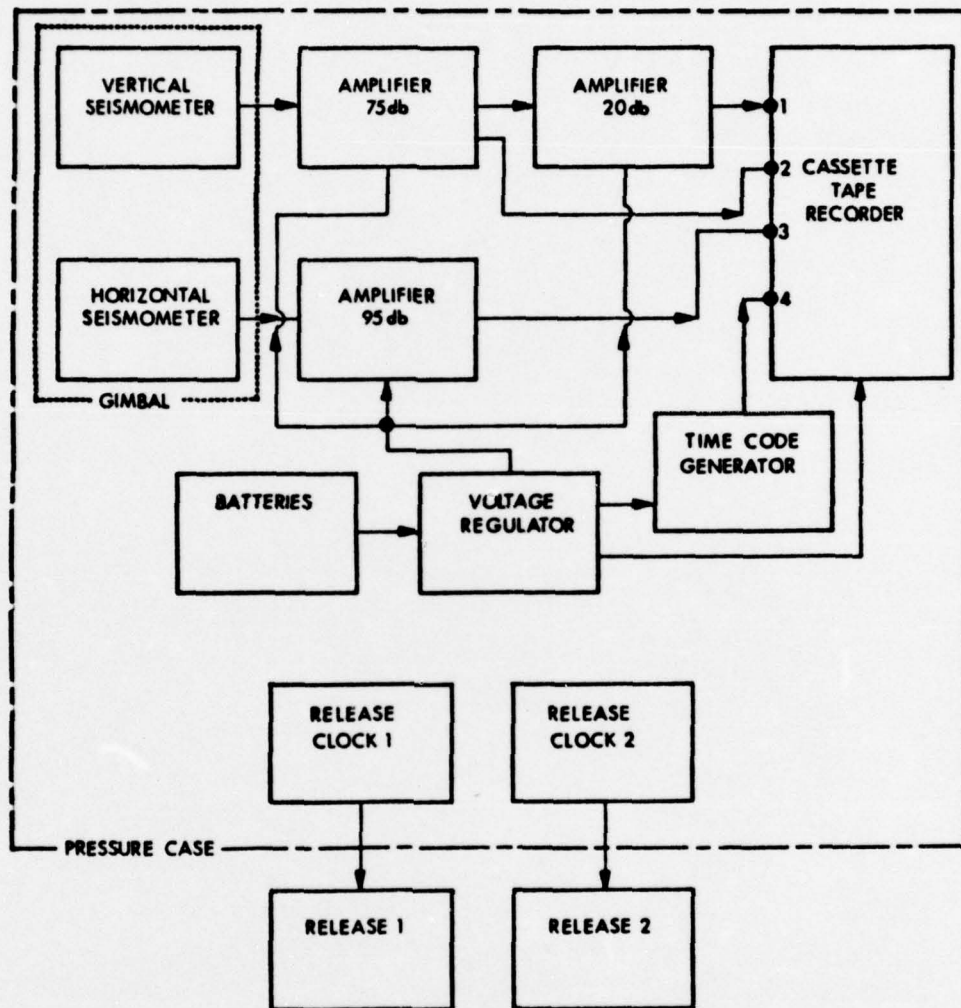
Fig. 3. Block diagram of ocean bottom seismograph.
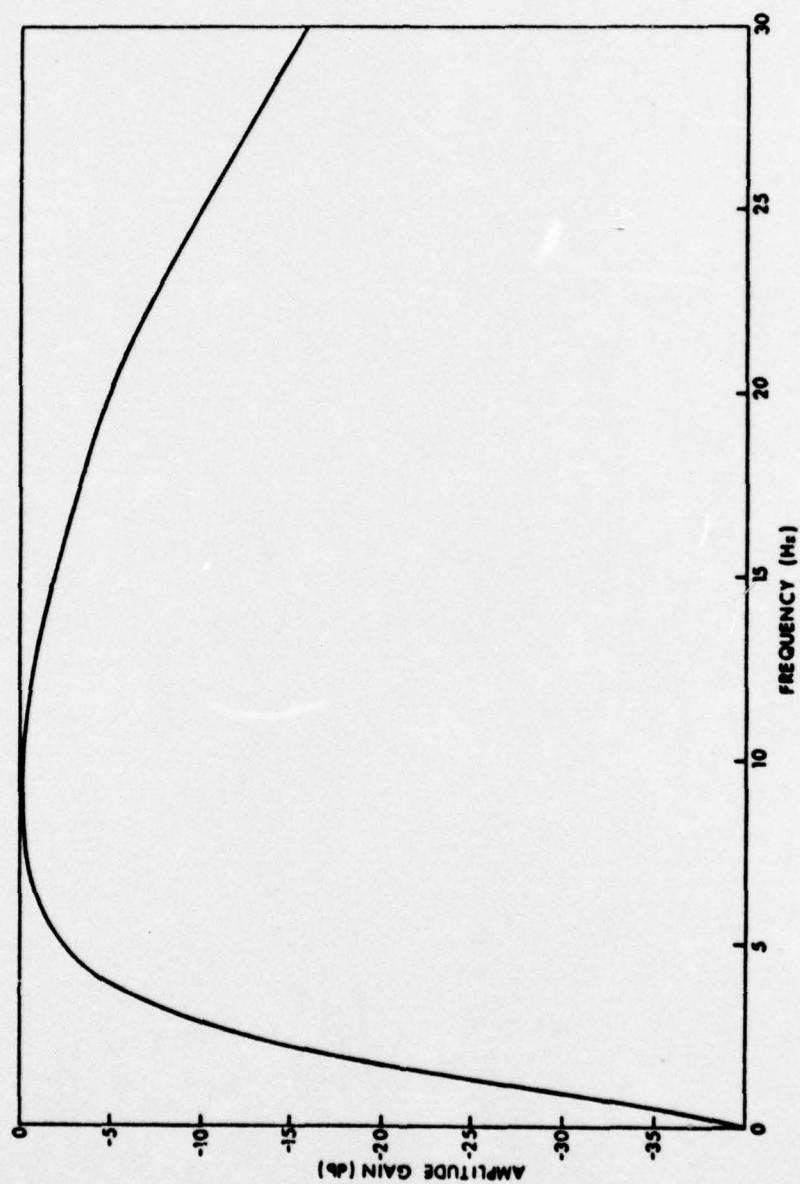
Fig. 4. Estimated response curve for geophone, amplifier, tape recording system, and playback system.
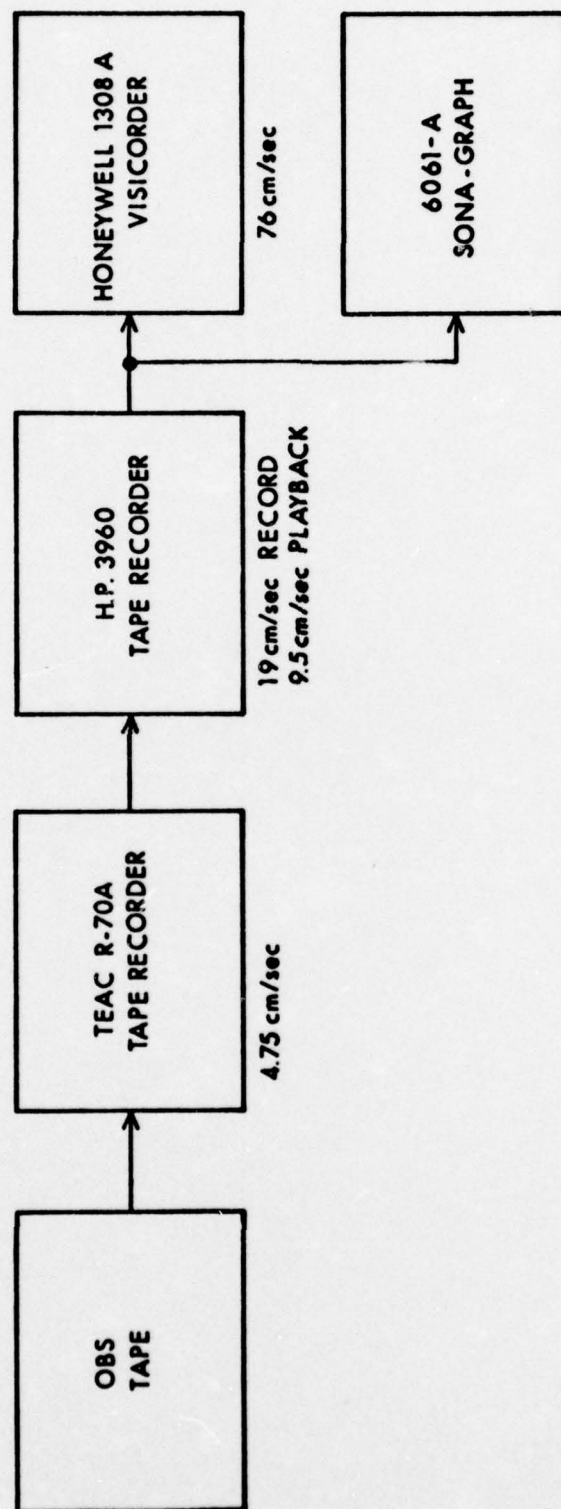
Fig. 5. Playback scheme. Time compression ratios for original OBS tape recording and Hewlett-Packard 3960 playback are 1:400 and 1:200, respectively.
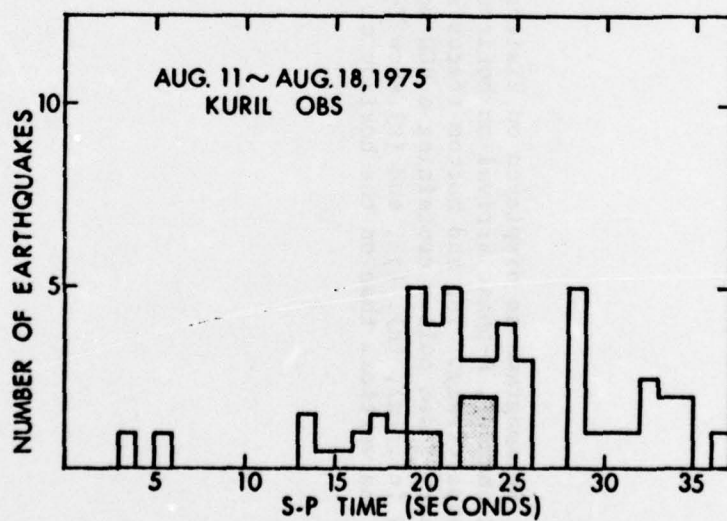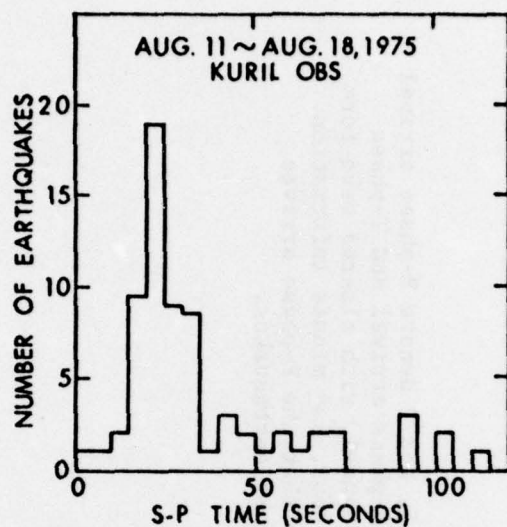
Fig. 6. S-P time distribution for (a) all detected earthquakes
and (b) those with S-P time between 0 and 37 seconds. Shaded area
indicates those earthquakes accompanied by T-phase activity.

Fig. 7. Seismograms as displayed on Visicorder. P, P_1, S, and T denote P-phase arrival on vertical channel, P-phase arrival on horizontal channel, S-phase arrival and T-phase arrival, respectively. Top and bottom traces are the time channel, with altered wave form of the primary 1-sec pulses containing a BCD code with day, hour, and minute information. Earthquakes (c), (g), (h), (j), and (k) show T-phases. Note that the P-phase arrives earlier on the vertical than on the horizontal channel for most earthquakes.
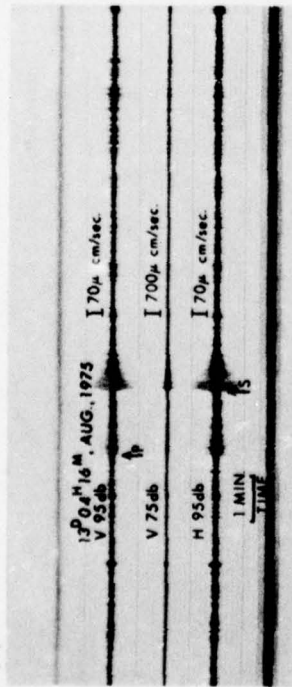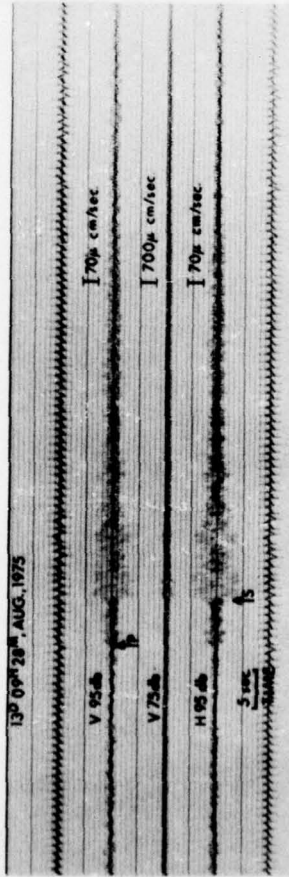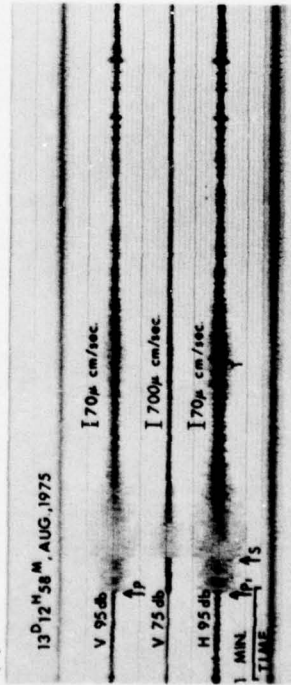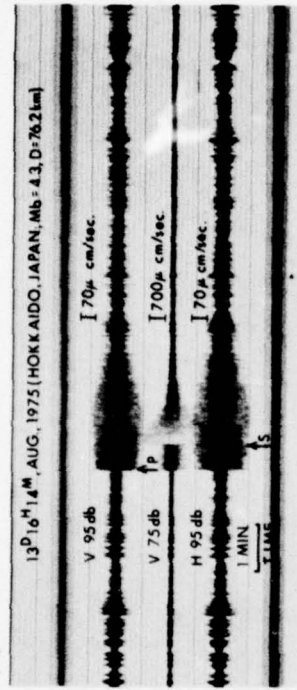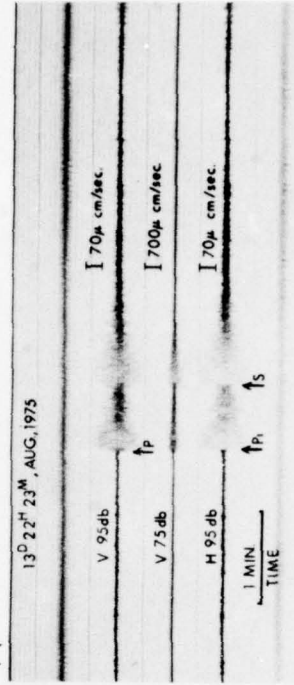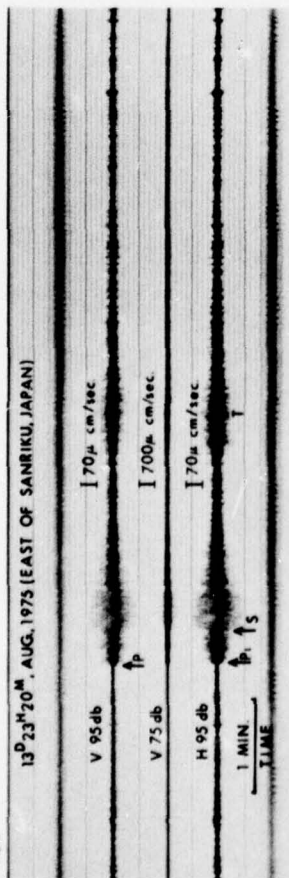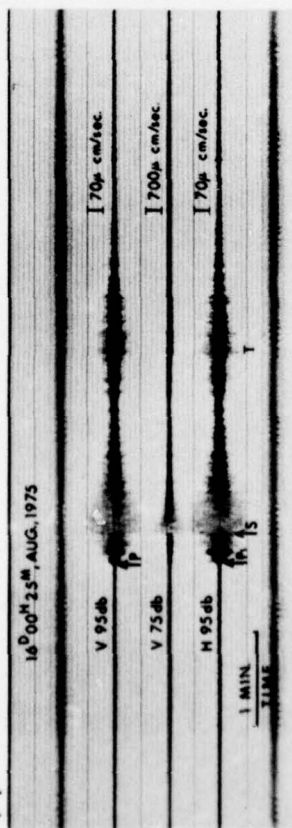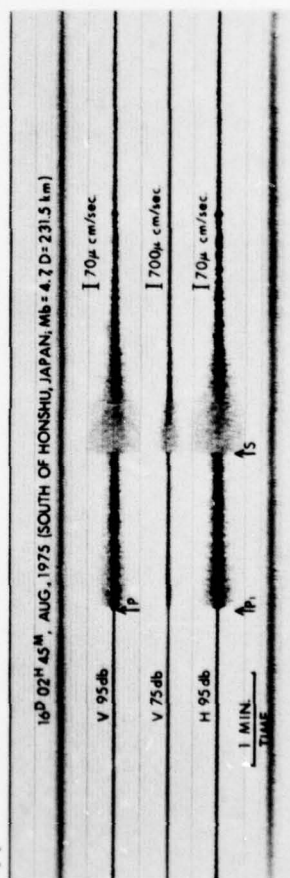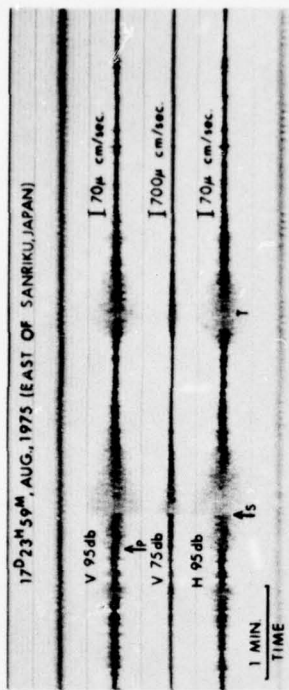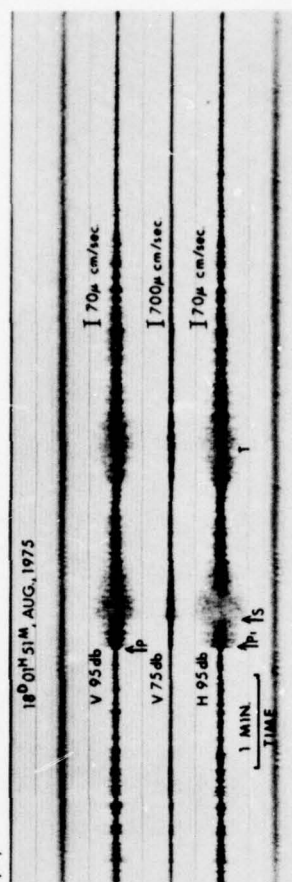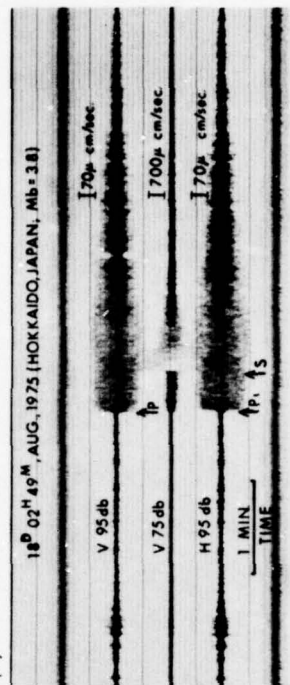
Fig. 7.

Fig. 7. (continued)
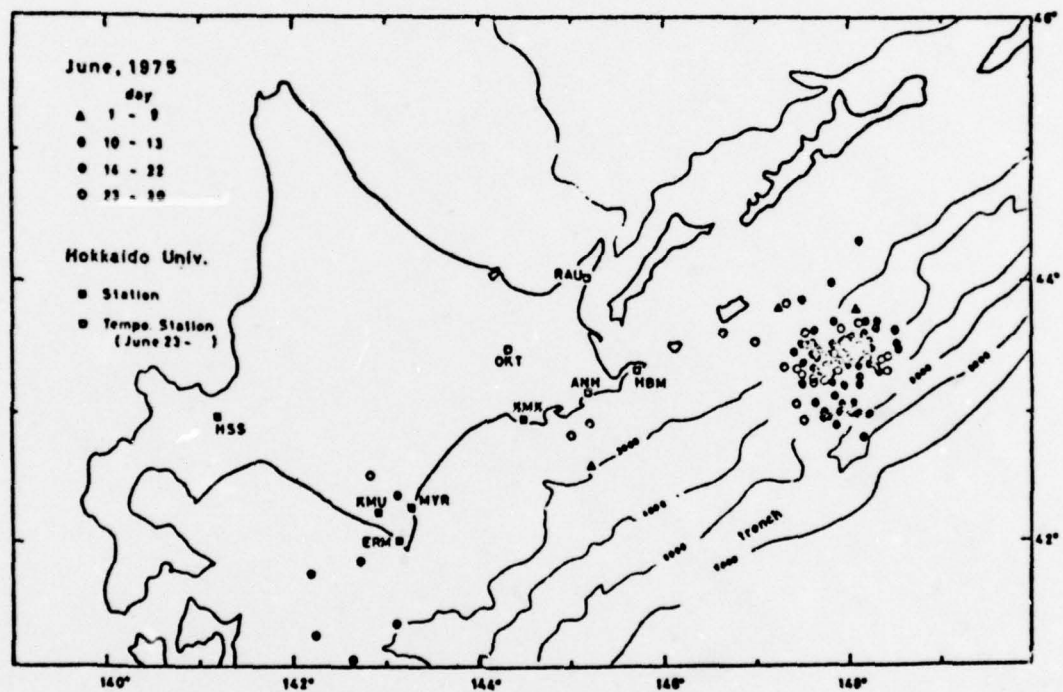
Fig. 8. Epicentral distribution of aftershocks of the 10 June
and 13 June 1975 earthquakes (after Japan, Hokkaido University, 1976).
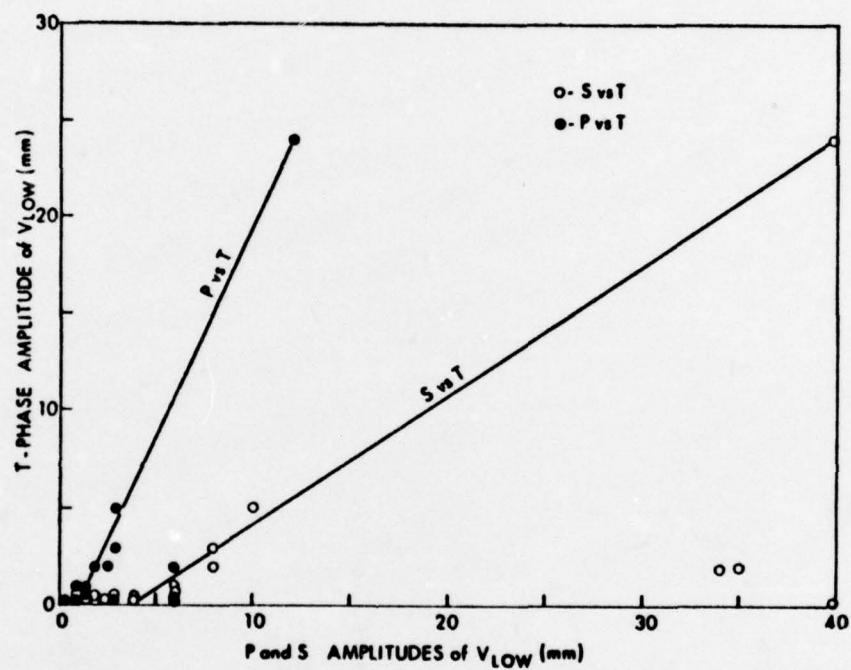
Fig. 9. T-phase amplitude versus P and S wave amplitudes as recorded on the low-gain vertical channel for all earthquakes with S-P time between 19 and 24 seconds. T-phase generating earthquakes occurred in the aftershock region of the 10 June and 13 June 1975 earthquakes and near the Japan Trench.
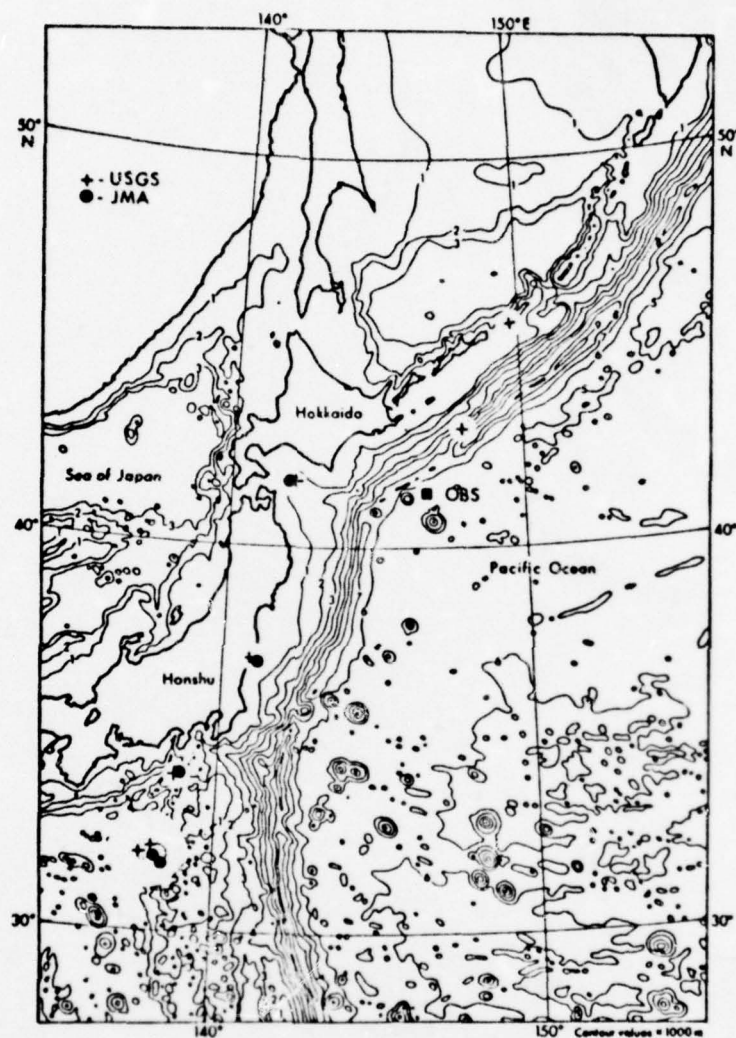
Fig. 10. Chart showing epicenters of the seven earthquakes used
in the present analysis, as determined by the Japan Meteorological
Agency and the U.S. Geological Survey.
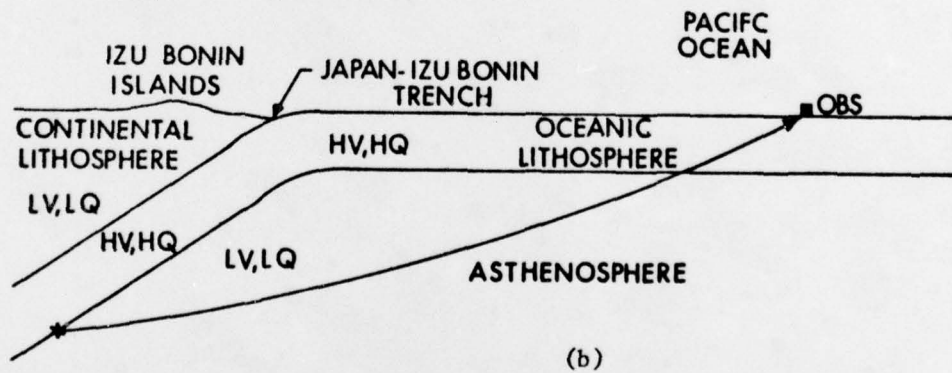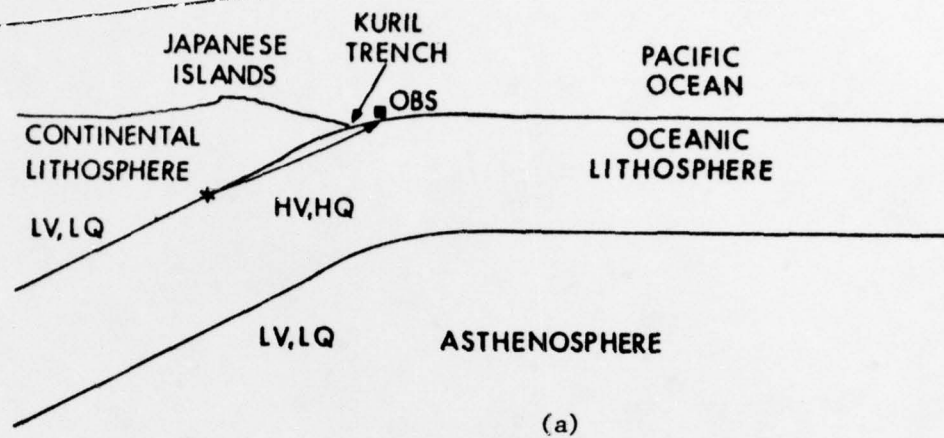
Fig. 11. Schematic ray paths from the hypocenter to the OBS for (a) earthquakes with negative travel time anomalies and (b) earthquakes with normal arrivals. The ray path for (a) lies entirely in the high velocity (HV), high Q (HQ) zone, whereas for (b), the path lies predominantly in the low velocity (LV), low Q (LQ) zone.
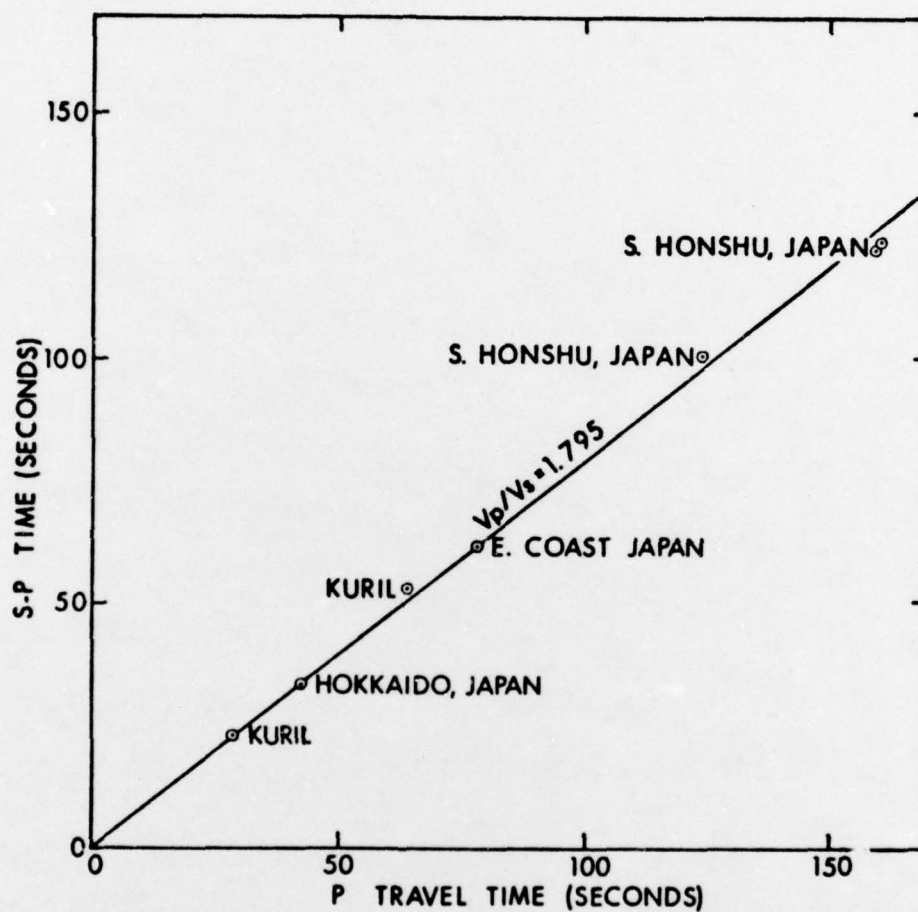
Fig. 12. S-P time versus P arrival time for the OBS, vertical channel, using U.S. Geological Survey epicenter determinations.
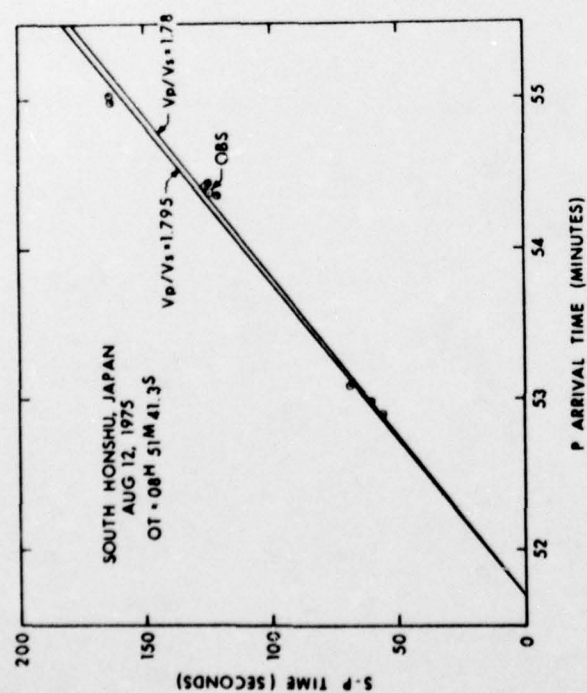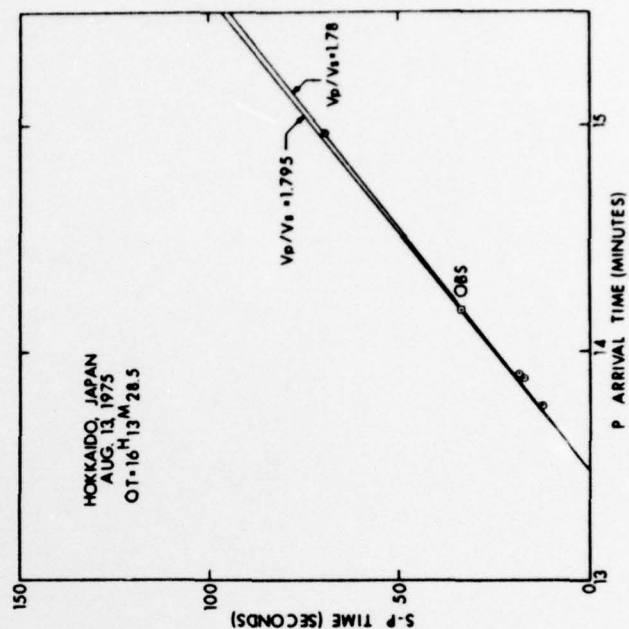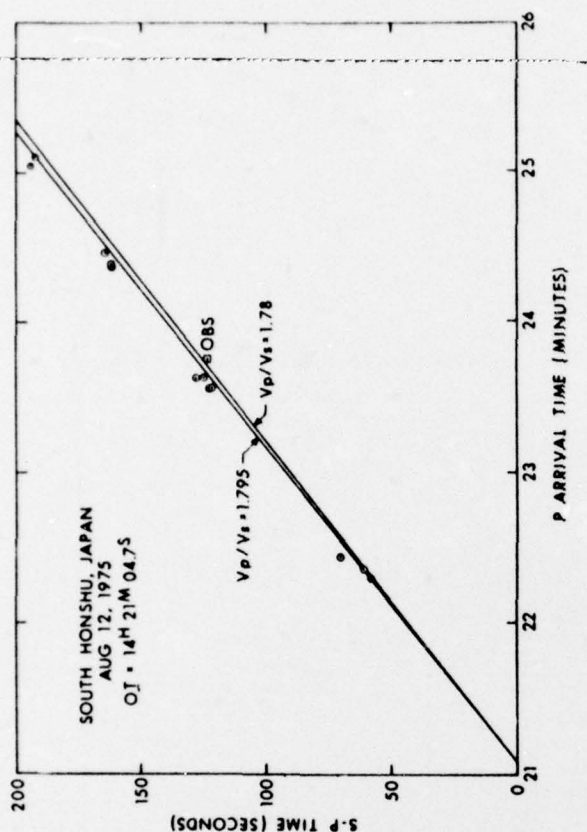
Fig. 13. S-P time versus P arrival time for individual earthquakes, using U. S. Geological Survey epicenter determinations. Land station arrivals are denoted by circles, OBS arrivals by squares.
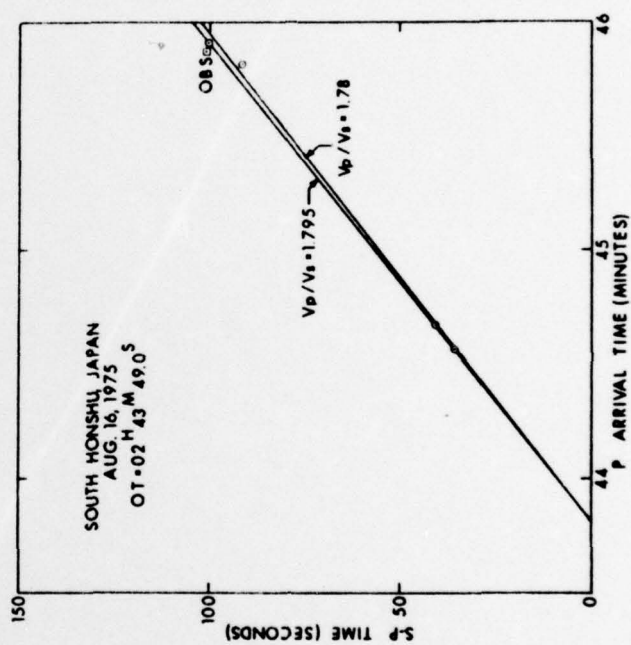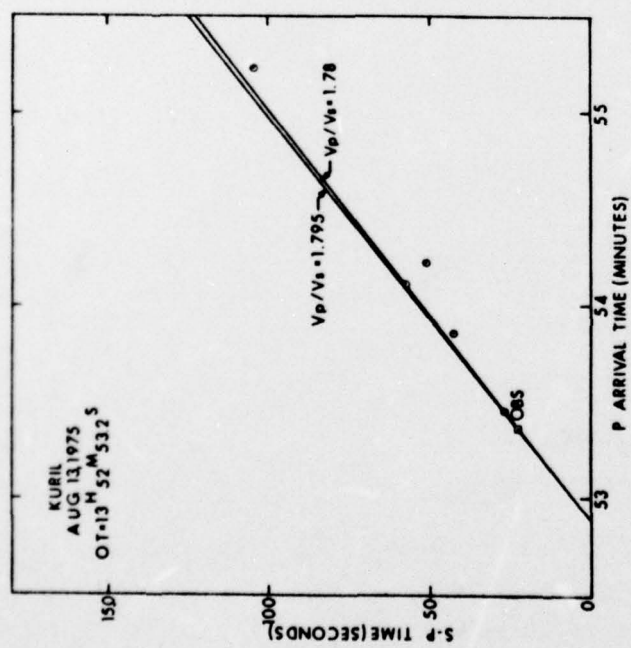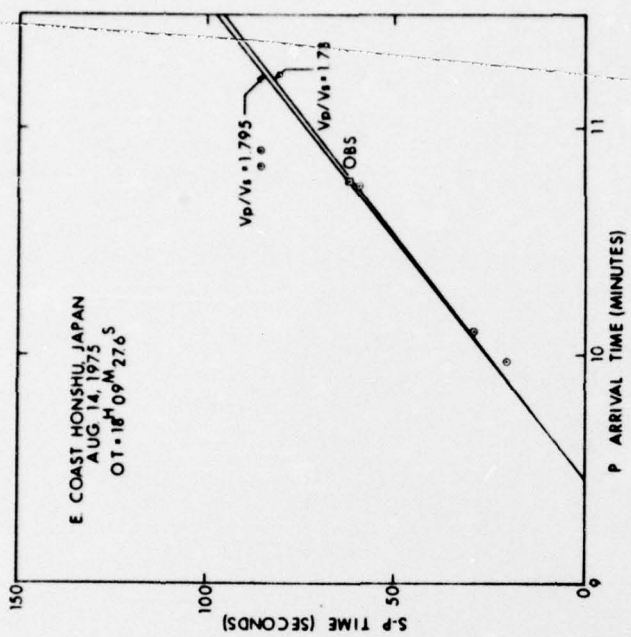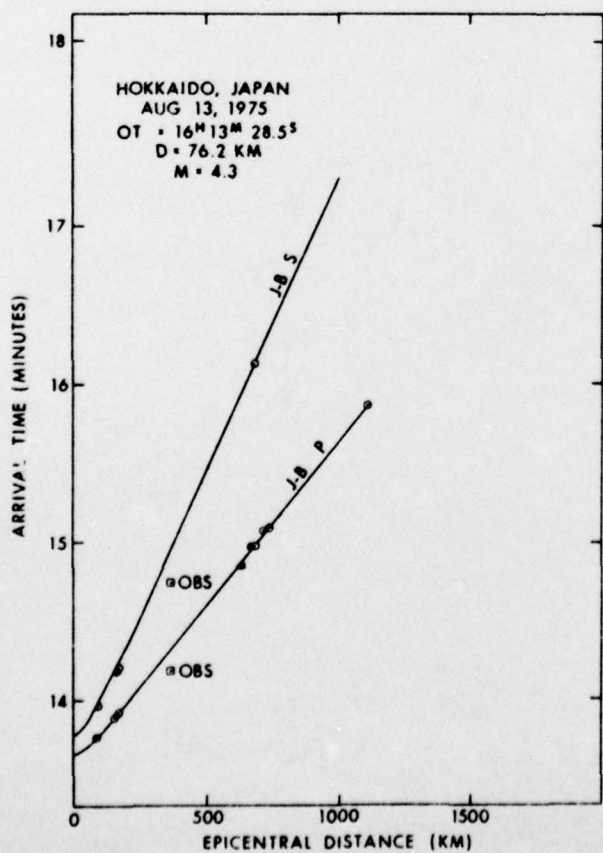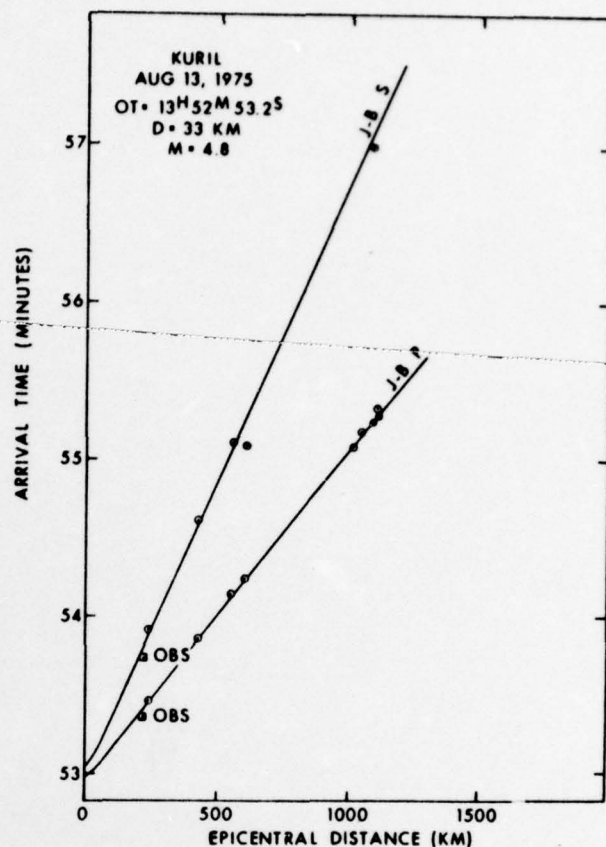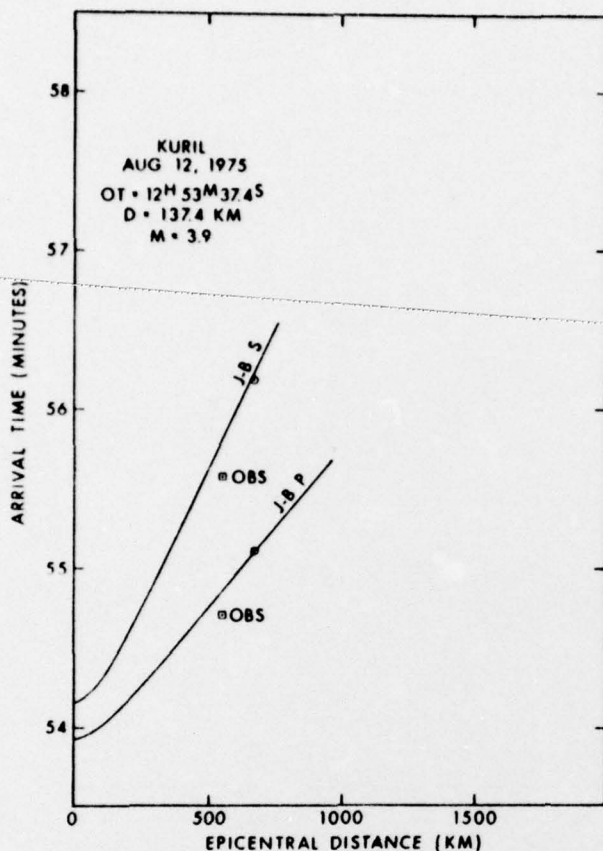
Fig. 13 (cont.)

Fig. 14. Travel time curves for earthquakes with early OBS arrivals. Land station arrivals are denoted by circles, OBS arrivals by squares. The solid lines represent standard Jeffreys-Bullen travel time curves.

NEAR E COAST
HONSHU, JAPAN
AUG 14, 1975
OT = 18^H 09^M 27.6^S
D = 52.0 KM
M = 5.5

NEAR S COAST
HONSHU, JAPAN
AUG 16, 1975
OT = 2^H 43^M 49.0^S
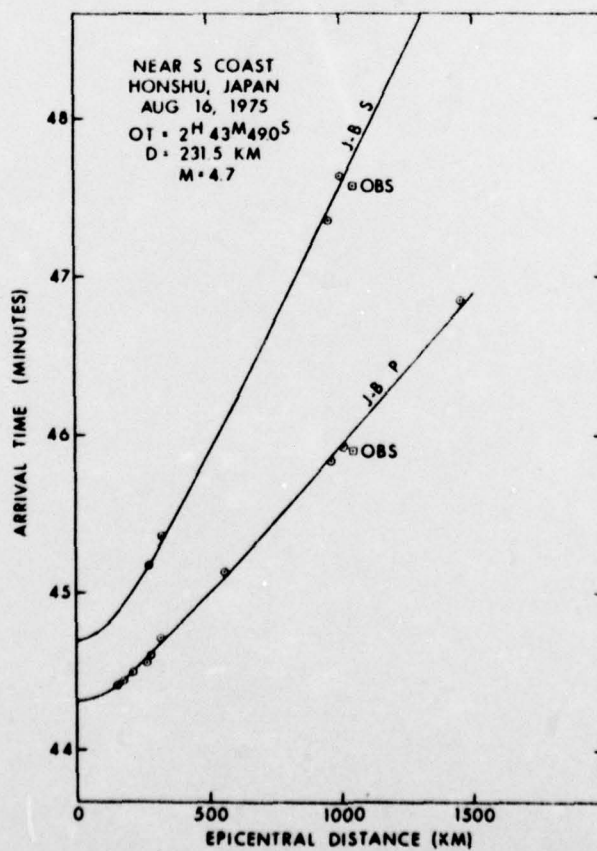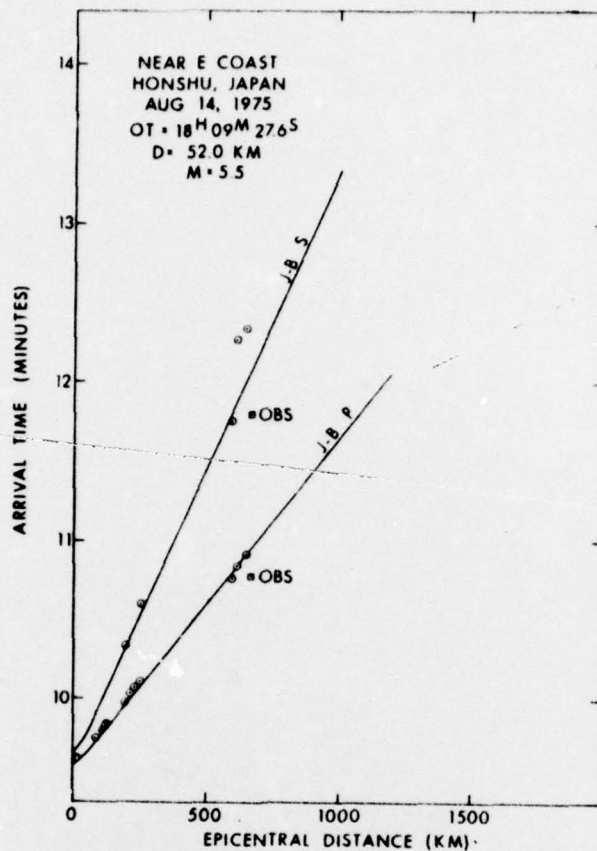D = 231.5 KM
M = 4.7

Fig. 14 (cont.)
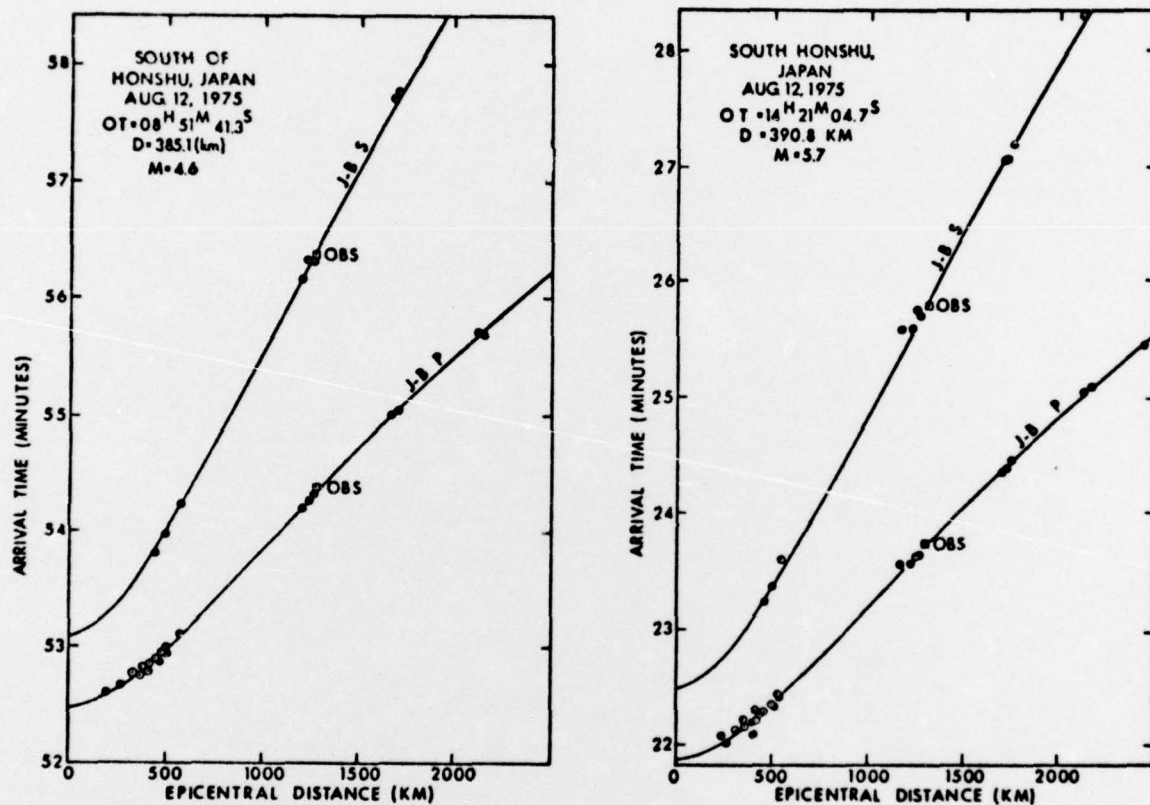
Fig. 15. Travel time curves for earthquakes with normal OBS arrivals. Symbols are the same as in Fig. 14.
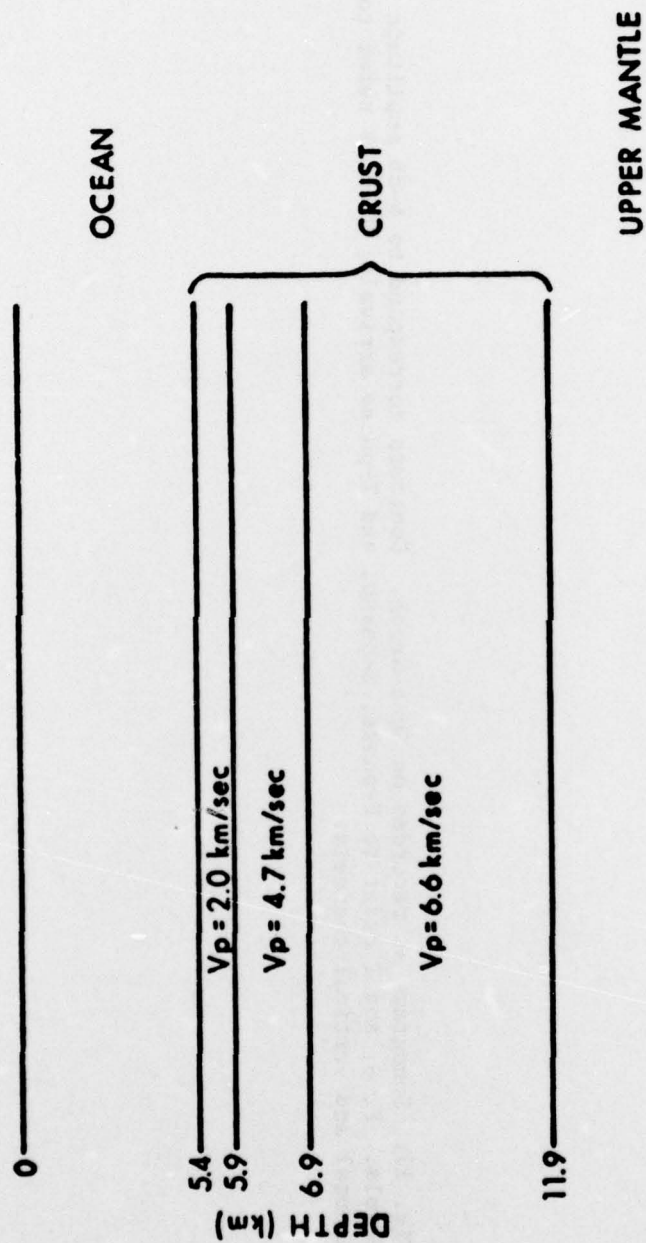
Fig. 16. Crustal model used to calculate average mantle velocities, based on the results of *Ludwig et al.* [1966] and *Den et al.* [1971].

Fig. 17. Sonograms as recorded on Sona-Graph. Contours correspond to 6-db amplitude intervals. P, S, and T refer to P-phase, S-phase, and T-phase arrivals; H and V refer to horizontal and vertical channels.

Fig. 17

Fig. 19. Q variation as a function of S-P time. The ordinate refers to the slope of logarathmic amplitude decay with frequency. The solid and dotted lines are calculated using a model with a flat velocity amplitude source spectrum with varying Q for P and S waves, respectively.

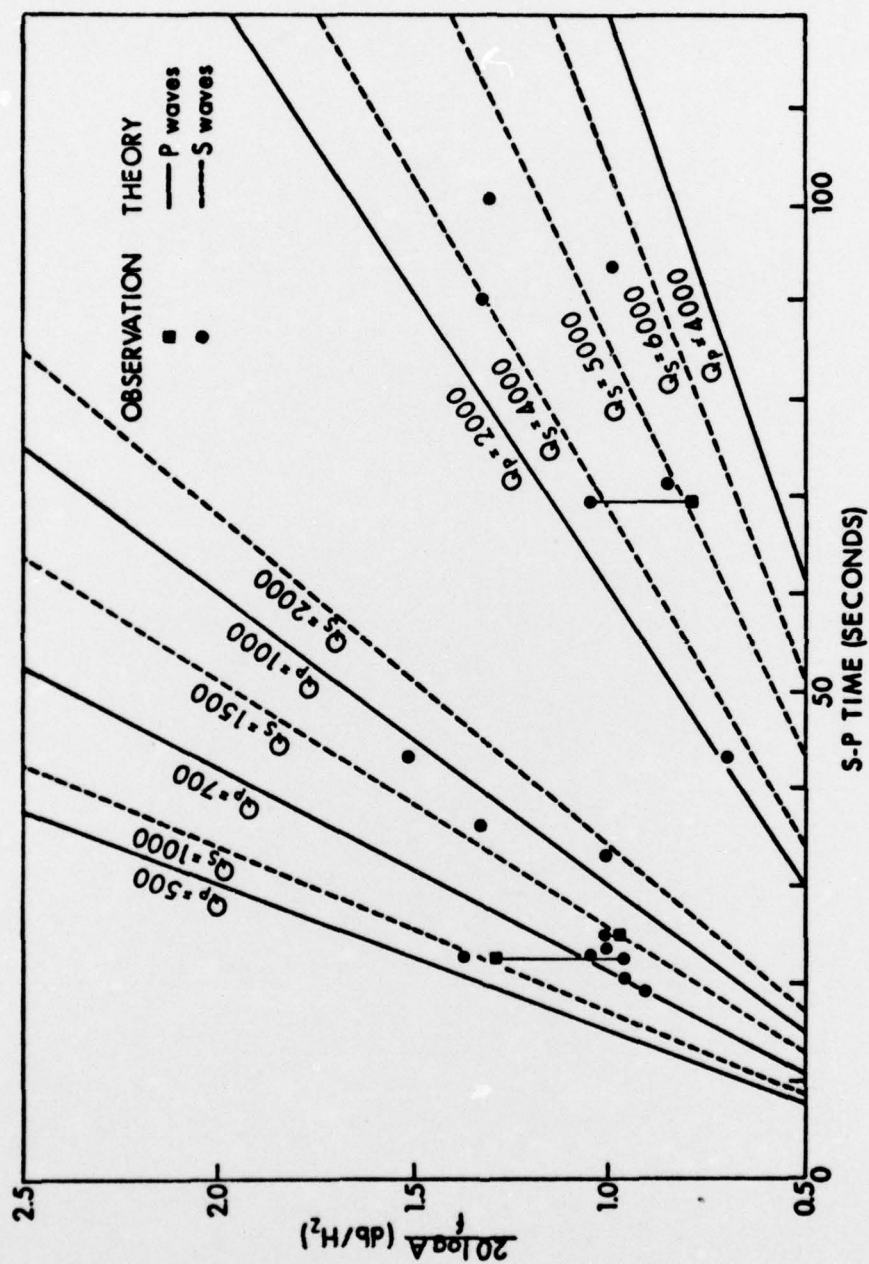| REPORT DOCUMENTATION PAGE		READ INSTRUCTIONS BEFORE COMPLETING FORM
1. REPORT NUMBER HIG-76-9	2. GOVT ACCESSION NO.	3. RECIPIENT'S CATALOG NUMBER
4. TITLE (and Subtitle) OCEAN BOTTOM SEISMOMETER STUDY OF THE KURIL TRENCH AREA		5. TYPE OF REPORT & PERIOD COVERED
		6. PERFORMING ORG. REPORT NUMBER HIG-76-9
7. AUTHOR(s) Junzo Kasahara and Robert R. Harvey		8. CONTRACT OR GRANT NUMBER(s) N00014-75-C-0209
9. PERFORMING ORGANIZATION NAME AND ADDRESS Hawaii Institute of Geophysics 2525 Correa Road Honolulu, HI 96822		10. PROGRAM ELEMENT, PROJECT, TASK AREA & WORK UNIT NUMBERS
11. CONTROLLING OFFICE NAME AND ADDRESS Office of Naval Research Ocean Science and Technology Division Arlington, VA 22217		12. REPORT DATE August 1976
		13. NUMBER OF PAGES -64-
14. MONITORING AGENCY NAME & ADDRESS(if different from Controlling Office) Office of Naval Research Branch Office 1030 East Green Street Pasadena, CA 91106		15. SECURITY CLASS. (of this report) Unclassified
		15a. DECLASSIFICATION/DOWNGRADING SCHEDULE

16. DISTRIBUTION STATEMENT (of this Report)

Approved for public release; distribution unlimited

17. DISTRIBUTION STATEMENT (of the abstract entered in Block 20, if different from Report)

NOAA-JTRE 166

18. SUPPLEMENTARY NOTES

Joint technical report with Joint Tsunami Research Effort, Pacific Marine Environmental Laboratory, Environmental Research Laboratories, NOAA. NOAA-JTRE Report NOAA-JTRE-166.

19. KEY WORDS (Continue on reverse side if necessary and identify by block number)

Seismology
Tsunamis
OBS
Joint Soviet-American Tsunami Expedition

20. ABSTRACT (Continue on reverse side if necessary and identify by block number)

An ocean bottom seismograph was deployed on the seaward side of the Kuril Trench off Hokkaido, Japan, in 5460 m of water, in August, during the 1975 joint Soviet-American Tsunami Expedition. During the seven-day record, S-P times were distributed in three groups: 19-24 sec, corresponding to aftershocks of the 10 June and 13 June 1975 earthquakes southeast of Nemuro, Japan and to earthquakes east of Sanriku, Japan; ~30 sec, from south of Erimo Peninsula, Hokkaido; and ~100 sec, from the Izu-Bonin Islands. Seven earthquakes, with hypocenters well determined by the land seismic net, are studied in → (cont.)

DD FORM 1 JAN 73 1473 EDITION OF 1 NOV 65 IS OBSOLETE
S/N 0102-014-6601 |

164400

20. ABSTRACT (cont.)

detail. A shallow focus earthquake yields typical oceanic mantle velocities shallower than 50 km in the slab which dips under the Japanese archipelago. However, deeper focus earthquakes reveal anomalously high velocities $(V_p \geq 8.50$ km/sec, $V_s \geq 4.80$ km/sec) averaged over the upper 230 km, in agreement with the models of Utsu and Oliver and Isacks. Two deep earthquakes, whose paths lie in the Pacific Ocean asthenosphere, suggest a velocity 3% lower than that predicted by Jeffreys-Bullen, in agreement with the above models. Spectral analysis of S arrivals suggests Q_s values of 1000-1500 for nearby earthquakes (S-P < 43 sec) and 4000-6000 for longer-distance earthquakes, implying an unusual attenuation mechanism for long travel paths, which enhances the high frequencies.

MANDATORY DISTRIBUTION LIST

FOR UNCLASSIFIED TECHNICAL REPORTS, REPRINTS, & FINAL REPORTS
PUBLISHED BY OCEANOGRAPHIC CONTRACTORS
OF THE OCEAN SCIENCE AND TECHNOLOGY DIVISION
OF THE OFFICE OF NAVAL RESEARCH
(REVISED JAN 1975)

1   Director of Defense Research   12** Defense Documentation
    and Engineering   Center
    Office of the Secretary of Defense   Cameron Station
    Washington, D. C.   20301   Alexandria, Virginia
    ATTN: Office, Assistant Director   22314
           (Research)

    Office of Naval Research   Commander
    Arlington, Virginia   22217   Naval Oceanographic
3   ATTN: (Code 480)*   Office
1   ATTN: (Code 460)   Washington, D. C.   20390
1   ATTN: (Code 102-OS)   1   ATTN: Code 1640
6   ATTN: (Code 102IP)   1   ATTN: Code 70

1 ONR ResRep (if any)   1   NODC/NOAA
                                                     Rockville, MD   20882

    Director
    Naval Research Laboratory
    Washington, D. C.   20375
6   ATTN: Library, Code 2620

TOTAL REQUIRED - 35 copies

* Add one separate copy of   ** Send with these 12 copies
   Form DD-1473   two completed forms DDC-50,
                                          one self addressed back to
                                          contractor, the other ad-
                                          dressed to ONR, Code 480